Atmos. Chem. Phys., 10, 5719–5738, 2010
www.atmos-chem-phys.net/10/5719/2010/
doi:10.5194/acp-10-5719-2010

Atmospheric Chemistry and Physics

Impact of West African Monsoon convective transport and lightning NO_x production upon the upper tropospheric composition: a multi-model study

B. Barret[1,2], J. E. Williams[3], I. Bouarar[4], X. Yang[5], B. Josse[6], K. Law[4], M. Pham[4], E. Le Flochmoën[1,2], C. Liousse[1,2], V. H. Peuch[6], G. D. Carver[5], J. A. Pyle[5], B. Sauvage[1,2], P. van Velthoven[3], H. Schlager[7], C. Mari[1,2], and J.-P. Cammas[1,2]

[1]Laboratoire d'Aérologie/OMP, Université de Toulouse, Toulouse, France
[2]Laboratoire d'Aérologie, CNRS UMR 5560, Toulouse, France
[3]KNMI, De Bilt, The Netherlands
[4]LATMOS/IPSL, UPMC, Paris, France
[5]Centre for Atmospheric Science and Department of Chemistry, University of Cambridge, Cambridge, UK
[6]CNRM-GAME, Météo-France and CNRS URA 1357, Toulouse, France
[7]Institut für Physik der Atmosphäre, Deutsches Zentrum fur Luft- und Raumfahrt (DLR), Oberpfaffenhofen, Germany

Received: 22 December 2009 – Published in Atmos. Chem. Phys. Discuss.: 1 February 2010
Revised: 25 May 2010 – Accepted: 11 June 2010 – Published: 30 June 2010

Abstract. Within the African Monsoon Multidisciplinary Analysis (AMMA), we investigate the impact of nitrogen oxides produced by lightning ($LiNO_x$) and convective transport during the West African Monsoon (WAM) upon the composition of the upper troposphere (UT) in the tropics. For this purpose, we have performed simulations with 4 state-of-the-art chemistry transport models involved within AMMA, namely MOCAGE, TM4, LMDz-INCA and p-TOMCAT. The model intercomparison is complemented with an evaluation of the simulations based on both spaceborne and airborne observations. The baseline simulations show important differences between the UT CO and O_3 distributions simulated by each of the 4 models when compared to measurements from the MOZAIC program and fom the Aura/MLS spaceborne sensor. We show that such model discrepancies can be explained by differences in the convective transport parameterizations and, more particularly, the altitude reached by convective updrafts (ranging between ∼200–125 hPa). Concerning UT O_3, the models exhibit a good agreement with the main observed features. Nevertheless the majority of models simulate low O_3 concentrations compared to both MOZAIC and Aura/MLS observations south of the equator, and rather high concentrations in the Northern Hemisphere. Sensitivity studies are performed to quantify the effect of deep convective transport and the influence of $LiNO_x$ production on the UT composition. These clearly indicate that the CO maxima and the elevated O_3 concentrations south of the equator are due to convective uplift of air masses impacted by Southern African biomass burning, in agreement with previous studies. Moreover, during the WAM, $LiNO_x$ from Africa are responsible for the highest UT O_3 enhancements (10–20 ppbv) over the tropical Atlantic between 10° S–20° N. Differences between models are primarily due to the performance of the parameterizations used to simulate lightning activity which are evaluated using spaceborne observations of flash frequency. Combined with comparisons of in-situ NO measurements we show that the models producing the highest amounts of $LiNO_x$ over Africa during the WAM (INCA and p-TOMCAT) capture observed NO profiles with the best accuracy, although they both overestimate lightning activity over the Sahel.

Correspondence to: B. Brice
(barp@aero.obs-mip.fr)

Published by Copernicus Publications on behalf of the European Geosciences Union.

1 Introduction

In the tropics the high humidity, strong insolation and significant emission of trace gas species from (e.g.) biomass burning (BB) results in a chemical environment which has a high degree of photochemical activity and plays a dominating role towards determining the atmospheric lifetime of important greenhouse gases and pollutants. The composition of the tropical free troposphere is driven by deep convection of trace gases and chemical pre-cursors emitted at the surface, as well as associated processes such as convective mixing, wet scavenging and subsequent deposition of hydrophilic compounds (e.g., Mari et al., 2000), biogenic activity (e.g., Williams et al., 2009a) and NO_x production by lightning ($LiNO_x$) (e.g., Bond et al., 2002). The African continent is considered to be the region with the strongest lightning activity (Christian et al., 2003). According to Marufu et al. (2000), Africa is also the most important region concerning BB related O_3 with a contribution of 35% of the global production related to this source. Therefore, Africa plays a major role in controling the distribution of tropical tropospheric O_3 columns. This distribution is characterised by a persistent zonal Wave-1 pattern with maxima over the Atlantic and minima over the Pacific (Thompson et al., 2000). Furthermore, the most elevated O_3 concentrations in the free troposphere are observed in the South Atlantic during the Northern African BB season in December–February leading to an apparent paradox (Thompson et al., 2000). Both phenomena have been attributed to a combination of upper tropospheric (UT) O_3 production by lightning, subsidence of UT air masses over the southern tropical Atlantic within the Walker circulation and transport of UT O_3 from northern midlatitudes by Martin et al. (2002). Combining spaceborne observations of the O_3 tropospheric column and of lightning, Jenkins and Ryu (2004) also suggest $LiNO_x$ from west and central Africa as the most probable source of elevated O_3 levels over the equatorial Atlantic (5° S–10° N) during June-July-August (JJA). One goal of the African Monsoon Multidisciplinary Analyses (AMMA; Redelsperger et al., 2006) is to quantify the most important processes that govern the chemical composition of the African troposphere (Mari et al., 2005; Reeves et al., 2010) and identify possible deficiencies in the performance of models used for this purpose. A number of previous studies related to the AMMA programme have brought new insight concerning the tropospheric chemistry active during the West African Monsoon (WAM). All these studies revealed well marked latitudinal distributions of chemicals both in the lower troposphere where they reflect the latitudinal organization of surface processes and associated emissions (Saunois et al., 2009) and in the UT due to the vertical and meridional circulations by the Hadley cells. Analysing regular airborne observations from the MOZAIC program, Sauvage et al. (2007a) have shown that the meridional transect of UT O_3 over Africa is characterized by a minimum that follows the Inter Tropical Convergence Zone (ITCZ). They attribute this latitudinal O_3 gradient to convective uplift of O_3 depleted air masses in the ITCZ, which then experience enhanced photochemical production in the upper branches of the Hadley circulation. From sensitivity runs with a 2-D vertical-meridional model Saunois et al. (2008) have highlighted the predominant role of both $LiNO_x$ and biogenic VOCs towards establishing the meridional gradient observed in the African UT. Interestingly, the AMMA experiment revealed a persistent influence of fires from the Southern Hemisphere upon the composition of the West African troposphere during the wet season (Sauvage et al., 2007a; Mari et al., 2008; Real et al., 2010).

In large-scale global Chemistry Transport Models (CTM's), convection and related processes such as wet scavenging and $LiNO_x$ production are typically represented by sub-grid parameterizations, resulting in important differences between models and thus uncertainties. Based on an ensemble of multi-model simulations including 26 state-of-the-art CTM's, Stevenson et al. (2006) have shown that the highest discrepancies concerning tropospheric O_3 occur in the tropical UT. From multi-model simulations, Rasch et al. (2000) have also shown that model differences are the strongest in the upper troposphere for species undergoing wet scavenging processes. Moreover, we note that there is an inconsistency in the literature concerning the influence of convective transport towards the global O_3 budget, where Lawrence et al. (2003) find there is a positive effect whereas Doherty et al. (2005) conclude the opposite. According to the recent overview concerning the contribution from lightning, Schumann and Huntrieser (2007) have provided a best estimate of the annually integrated global $LiNO_x$ source of 5 ± 3 Tg N/year, meaning that there is a large degree of uncertainty. This provides further motivation for performing a more in-depth analysis of the differences which occur between a typical sub-set of CTM's, in order to determine the most important factors involved.

The aim of our study is to quantify the impact of $LiNO_x$ production and convective mixing from the WAM upon the composition of the tropical UT during summer 2006. Exploiting novel components of the AMMA framework, it is based on simulations performed by the global CTM's that have participated in the AMMA multi-model intercomparison exercise (Williams et al., 2009b) and on the intense airborne AMMA measurement campaign that has been performed during July and August of 2006 (Reeves et al., 2010). Our study complements the study of (Williams et al., 2009b) who have already pointed to important differences concerning the representation of transport processes in the AMMA models based on passive tracers simulations and the study of Saunois et al. (2008) who based their UT O_3 budget on simplified 2-D simulations. In Sect. 2 we provide a brief description of each of the participating models. In Sect. 3 we present an overview of the observations against which the model results are compared and in Sect. 4 we discuss the

meteorological situation. In Sect. 5 we make an evaluation of convective transport from the different models based on the analysis of convective fluxes, and comparisons between simulated and observed CO and O_3 distributions. Sensitivity simulations are used to evaluate the impact of convective mixing upon the UT composition. Section 6 is dedicated to the analysis of the impact of $LiNO_x$ upon the tropical UT composition from the different models. The simulated distributions of lightning activity are evaluated with spaceborne observations and the simulated NO concentrations are compared to AMMA airborne observations. The impact of $LiNO_x$ upon tropospheric O_3 is quantified with sensitivity simulations. We summarize the discussions and present our final conclusions in Sect. 7.

2 Description of the models

Four different state-of-the-art global 3-D CTM's are employed in this study which include a diverse set of parameterizations for describing convection and advection, different vertical and horizontal resolutions and chemical mechanisms. In the following section we provide details concerning the emission inventories employed (Sect. 2.1), and briefly describe each of the participating CTM's in Sect. 2.2 to 2.5, where a summary is given in Table 1.

2.1 Surface emission inventory

For this experiment we adopt the global emission datasets defined within the EU-GEMS project (http://gems.ecmwf.int). These are based on a hybrid dataset assembled from the RETRO anthropogenic (http://retro.enes.org/) and GFEDv2 biomass burning (Van der Werf et al., 2006) emission datasets, which are both publicly available. For Africa, which is defined as the region between 20° W–40° E and 40° S–30° N, we apply the recently developed L3JRCv2 biomass burning and biofuel database (Liousse et al., 2009). Comparing BB emission totals for CO from Southern Africa provided in the L3JRCv2 inventory with the six different inventories shown in Bian et al. (2007) reveals that for JJA the values are higher than those commonly adopted in global CTMs for simulations. For instance, the total emission flux for CO in this region during JJA increases from 63 Tg CO to 165 Tg CO (not shown). Hence, the impact on the composition of the troposphere is potentially large. In order to evaluate this impact we also performed simulations with the GFEDv2 inventory over Africa.

2.2 MOCAGE

MOCAGE is the global CTM developed at the CNRM (Centre National de Recherches Meteorologiques) of Meteo-France (Bousserez et al., 2007; Teyssedre et al., 2007). The model is coupled off-line with the ECMWF meteorolgical analyses. The simulations are performed on a regular $2° \times 2°$ horizontal grid and on 47 hybrid (σ, P) levels from the surface up to 5 hPa. The vertical resolution typically varies from 40 to 400 m in the boundary layer (7 levels) and is about 800 m in the UTLS. The chemical scheme used is RACMOBUS, which combines the stratospheric scheme REPROBUS (Lefevre et al., 1994) and the tropospheric scheme RACM (Stockwell et al., 1997). Convective processes are simulated with the Kain-Fritsch-Bechtold's (KFB) scheme of Bechtold et al. (2001), and turbulent diffusion is calculated with the scheme by Louis (1979). The $LiNO_x$ parametrization is based on Mari et al. (2006). In this approach, once produced inside the convective column, NO_x molecules are redistributed by upward and downward transport and detrained in the environment and no a priori vertical placement of the emissions is prescribed. The Flash Frequencies (FF) are computed according to Price and Rind (1992) and the intra-cloud (IC) to cloud-ground (CG) lightning's ratio is computed according to Price and Rind (1993). Finally, we use the recommendation of Ridley et al. (2005) to prescribe a production of 2.2×10^{26} NO_x molecules by both IC and CG flashes. From this settings, we obtain a global annual emission of 3 Tg N yr^{-1} from lightning.

2.3 LMDz-INCA

LMDz4-INCA couples the Laboratoire de Meteorologie Dynamique General Circulation Model (GCM) LMDz version 4, and the Interaction with Chemistry and Aerosols (INCA) module (Hauglustaine et al., 2004). Model simulations, nudged towards ECMWF winds, were performed at a resolution of $2.5° \times 3.75°$. The model is composed of 19 vertical levels on sigma-p hybrid coordinates extending from the surface up to 3 hPa. This corresponds to a vertical resolution of about 300–500 m in the planetary boundary layer (first level at 70 m height) and to a resolution of about 2 km at the tropopause (with 7–9 levels located in the stratosphere). The large-scale advection of tracers is based on the finite volume transport scheme of Van Leer (1977) as discribed in Hourdin and Armengaud (1999). Deep convection is parameterized according to the Emmanuel's scheme (Emanuel, 1991, 1993) as described in Hourdin et al. (2006). LMDzINCA accounts for emissions, transport, photochemical transformations, and scavenging (dry deposition and washout) of chemical species. The model version used includes detailed VOC chemistry. $LiNO_x$ are parametrized according to Jourdain and Hauglustaine (2001) with FF based on Price and Rind (1992) for both marine and continental thunderstorms. Pickering et al. (1998) is used for vertical redistribution of lightning NOx. The IC/IG ratio is computed according Price and Rind (1993). According to Price et al. (1997), IC flashes produce 6.7×10^{25} and CG flashes 6.7×10^{26} NO molecules. The FF have been scaled by a constant factor in order to obtain a global annual emission of 5 Tg N yr^{-1}.

Table 1. Models settings.

	MOCAGE	TM4	INCA	p-TOMCAT
Horizontal resolution	2°×2°	3°×2°	2.5°×3.75°	2.8°×2.8°
vertical levels	47	34	19	31
Convection	Bechtold et al. (2001)	Tiedtke et al. (1989)	Emanuel (1991)	Tiedtke et al. (1989) +update (see text)
$LiNO_x$	Mari et al. (2006)	Meijer et al. (2001)	Jourdain and Hauglustaine (2001)	Stockwell et al. (1999)
FF's	CTH Price and Rind (1992)	Convective Rain Meijer et al. (2001)	CTH Price and Rind (1992)	CTH Price and Rind (1992)
IC/CG	Price and Rind (1993)	Price and Rind (1993)	Price and Rind (1993)	Price and Rind (1993)

2.4 TM4

TM4 is a 3-D CTM coupled off-line to ECMWF meteorological fields. The model was run at a horizontal resolution of 3°×2° with 34 vertical layers, with high resolution in the UTLS resulting in vertical layers of 1 km depth between 10–15 km. The model includes NMHC chemistry, and appropriate modules for sulphate and aerosol chemistry. A detailed description of the overall structure of the model is given in Dentener et al. (2003). All rate parameters and scavenging co-efficients have recently been updated using the latest recommendations as given in either Sander et al. (2006) or Yarwood et al. (2005). The version adopted here is identical to TM_4_AMMA used in Williams et al. (2009b). Moreover, parameterizations have also recently been included to provide a better description for cirrus particles (Fu, 1996; Heymsfield and McFarquhar, 1996). Convective tracer transport is calculated with a mass flux scheme that accounts for shallow, mid-level and deep convection (Tiedtke et al., 1989). Turbulent vertical transport is calculated by stability dependent vertical diffusion (Louis, 1979). The $LiNO_x$ production is parametrized according to Meijer et al. (2001) using a linear relationship between lightning flashes and convective precipitation. The total annual production is normalised to approximately 5 Tg N/yr. Marine lightning is prescribed to be ten times less active than continental lightning (Schumann and Huntrieser, 2007). The fraction CG/IC is fixed according to Price and Rind (1993). NO_x production per IC and CG flash is according to Price et al. (1997) and the vertical NO_x profile for injection of $LiNO_x$ into the model is an approximation of the "outflow" profile suggested by Pickering et al. (1998).

2.5 p-TOMCAT

The p-TOMCAT global CTM has a horizontal resolution of 2.8°×2.8° and 31 vertical levels from the surface up to 10 hPa. It integrates a tropospheric chemistry scheme (the ASAD chemical modelling software Carver et al., 1997) with more than 60 trace constituents on hybrid pressure levels, using an advection scheme conserving second-order moments (Prather, 1986). The horizontal transport and vertical mixing of tracers is based on 6-h meteorological fields, including winds and temperature, derived from the ECMWF operational analyses. Vertical mixing is based on a non-local scheme documented in Wang et al. (1999), which has been tested by Stockwell et al. (1997) by comparison with observed profiles of radon. The wet and dry deposition schemes used in the model have been tested by Giannakopoulos et al. (1999). Vertical transport of chemical species by moist convection is based on the scheme from Tiedtke et al. (1989). By comparing with satellite data, it was found that the original implementation of Tiedke convective scheme used in p-TOMCAT could result in significantly underestimated convective cloud top height, especially in the tropical regions, because the driving meteorological analyses have already been convectively adjusted. To overcome this problem, the entrainment/detrainment rates were adjusted to use half the rates suggested in Tiedtke et al. (1989). A smaller entrainment rate means reducing the mixing of much stable environmental air into the cloud and thus maintaining a positive buoyancy to higher altitude within the cloud. Satellite total cloud amount coverage Rossow et al. (ISCCP-D2 monthly mean dataset, at http://isccp.giss.nasa.gov/products/browsed2.html, 1996) was used instead of a constant value to give the fraction of saturated water vapor in each model gridbox to trigger cloud. This improves the distribution of cloud, particularly tropical deep convection relative to previous versions of p-TOMCAT. In the present study, detrainments are assumed to be at the cloud top layer rather than in each layer between cloud top and bottom as in the original version, allowing maximum uplift for tracers from the boundary layer. Precipitations are computed from each layer newly formed condensed liquid water. One goal of the present study is to evaluate those modifications of the Tiedtke's scheme in the p-TOMCAT CTM. The $LiNO_x$ parameterization for previous p-TOMCAT simulations is described in Stockwell et al. (1999). The FF are simulated according to Price and Rind (1992) and the IC/CG ratio according to Price and Rind

(1993). In this simulation however, according to Ridley et al. (2005), IC and GC flashes have the same NO production rate which is set to 3×10^{26} NO molecules per flash (Thery et al., 2000; De Caria et al., 2005). Those settings give better $LiNO_x$ distributions after the modifications applied to the convective parameterization described above. The FF are scaled to give an annual global emission of 3 Tg N in year 2006. Finally, CG emissions are distributed from the surface up to 500 hPa and IC emissions from 500 hPa to the cloud top. Further details about the model physical and chemical processes and its validation against observations can be found in Law et al. (1998); Stockwell et al. (1999); Wang et al. (1999); Yang et al. (2005).

3 Observations

3.1 MOZAIC observations

As part of the MOZAIC program, in-situ measurements of CO and O_3 have been performed daily from Windhoek (22.5° S, 17.5° E, Namibia) to Frankfurt (50° N, 8.6° E, Germany) since December 2005 with instruments onboard a regular Air-Namibia aircraft. MOZAIC measurements carried out with a 30 s response time and with a reported precision of ∼5 ppbv for CO (Nedelec et al., 2003) and 1 ppbv for O_3 (Thouret et al., 1998) have been averaged in 1 min time bins. For the comparisons, outputs from the model simulations have been interpolated to the 1 min averaged observation times and locations. We have selected data recorded at flight pressure levels smaller than 250 hPa in order to have sufficient data for statistical comparisons and to be close enough to the lowermost level (215 hPa) of the MLS observations.

3.2 AMMA airborne observations

During the AMMA campaign in July and August 2006, the tropospheric composition has been documented by a large number of observations from instrumented aircrafts. Here, we are using the NO observations from the ground up to the UT that have been carried out by the DLR Falcon 20 in order to evaluate the $LiNO_x$ representations in the four CTM's. These observations, described in Reeves et al. (2010), correspond to 6 flights carried out between 4 and 15 August 2006 from Ouagadougou between 8–17° N and between 10° W–3° E. The NO instrument operated on board the DLR Falcon use NO/O_3 chemiluminescence technique including a zero volume upstream of the detector reaction vessel (Schlager et al., 1997; Huntrieser et al., 1998). Sample air was passed from outside the aircraft boundary layer to the detector inside the aircraft cabin through a Teflon tube. The air mass flow was kept constant at 3 L/min (STP). During the flights the instrument was operated in different modes for measurement and calibration. The precision and accuracy of the NO measurements is 7% and 12%, respectively. The data have been segregated and grouped into a convective (CONV) and non-convective (NOCONV) class, depending on whether or not the sampled air masses have been freshly impacted by deep convection. The split between the two classes has been performed combining 3–4 days backtrajectories and observations of high altitude clouds from the MSG satellite (brightness temperatures less than 200 K). The method used here for observations by the DLR Falcon 20 is similar to the method described in (Law et al., 2010) concerning the observations by the M55 Geophysica. As for the MOZAIC observations, we have performed interpolations of the model outputs to the 1 min averaged NO observation times and locations.

3.3 Aura/MLS observations of O_3 and CO in the UTLS

The MLS instrument, flying onboard the Aura satellite since August 2004 is providing information about the vertical profiles of 17 atmospheric parameters retrieved from the millimeter and sub-millimeter thermal emission measured at the atmospheric limb (Waters et al., 2006). We use the latest MLS O_3 and CO observations (V2.2) described in Pumphrey et al. (2007). MLS is able to measure O_3 and CO in the UTLS (215, 147, 100 and 68 hPa) with a good spatial coverage in the tropical UT thanks to a low sensitivity of measurements in the millimeter and sub-millimeter domain to high humidity and clouds. MLS O_3 (resp. CO) data in the UT have a 3×200 km (resp. 4×500 km) vertical and along track resolution, a precision of 40 ppbv (resp. 20 ppbv) and a bias uncertainty of 20 ppbv (resp. 40 ppbv) (Livesey et al., 2007). Livesey et al. (2007) have made detailed characterization and validation of MLS CO and O_3 data in the UTLS and the observations used in our study have been screened according to their recommendations. Comparing MLS CO and MOZAIC in situ airborne CO observations at northern mid-latitude they show that MLS CO at 215 hPa is roughly a factor of 2 too high and they deduce a scaling uncertainty of ∼100% at that level. In their validation studies, Clerbaux et al. (2008) and Pumphrey et al. (2007) have compared CO profiles measured by the ACE-FTS (Bernath et al., 2005) and Aura/MLS instruments. They both show that MLS is biased high in the UT with the highest relative difference (∼100%) found around 12 km and that the bias is the lowest in the Lower Stratosphere (LS) around 18–20 km. Based upon the aforementioned validation studies, Barret et al. (2008) have estimated the biases of MLS CO observations at the 4 UTLS retrieval levels within the scaling uncertainties described in Livesey et al. (2007) using the ACE-FTS tropical CO climatology from Folkins et al. (2006) (see their Fig. 12). They have applied their adjustment based upon July 2006 tropical averages of the MLS data leading to an underestimation of the MLS/ACE-FTS ratio (1.6 at 215 hPa) because tropical CO exhibits a minimim during boreal summer. In order to improve the method, we have computed the ratio MLS/ACE-FTS based on MLS and ACE-FTS climatologies for the years 2004–2008. For the 215 hPa, of most interest in our study, we

found that tropical MLS CO data are higher than ACE-FTS data by a factor of 1.8 and we have corrected the MLS data accordingly.

4 Meteorological context

Convective transport, $LiNO_x$ production, and the transport and photochemistry of O_3, and chemical precursors of O_3, are closely linked to the regional meteorological situation. A comparison of the meteorological situation during the wet season in 2006 as compared with other years is given in Janicot et al. (2008). This section gives a brief summary of the main meteorological features characterizing the WAM. Figure 1 displays the horizontal and vertical ECMWF winds for both the lower and upper troposphere.

At 850 hPa, during the WAM, the south easterly trade winds are blowing over Southern Africa and the South Atlantic (Fig. 1b). Over the Gulf of Guinea those winds strongly diminish in strength and change into the south westerly monsoon flux. The convergence of the monsoon flux with the north easterly dry Harmattan winds at the Inter-Tropical Front (ITF) is linked to the westward propagation of Mesoscale Convective Systems (MCS) within the Inter-Tropical Convergence Zone (ITCZ). These are characterized by the low values of Outgoing Longwave Radiation (OLR) shown in Fig. 1. This westward propagation of the MCS is closely linked to the strength and position of the African Easterly Jet (AEJ), which is located at around 600 hPa and confined within 5–10° N. Over the Atlantic and West Africa, the ITCZ is centered at around 10° N and extends slightly to the south of the equator once over Central Africa. Studying Fig. 1a it is noticeable that the ECMWF model is simulating ascending large scale vertical winds at 250 hPa, which are closely following low OLR values. South of the ITCZ, between roughly the equator and 10° S, the vertical transport is characterised by strong ascending winds up to about 700 hPa (Fig. 1b). According to Sauvage et al. (2007b), these vertical winds are primarily caused by surface gradients in temperature and humidity, with the warm dry surface being located poleward and the cooler wet surface equatorward of the ITF. Furthermore, based on a case study, Sauvage et al. (2007b) have shown that during the WAM, the low-level circulation induced by these surface gradients is responsible for the uplift of biomass burning pollutants to the level of the African Easterly Jet (∼600 hPa), which results in their long-range transport to Western Africa. The large scale UT circulation is characterised by the presence of thermally induced anticyclones over low-latitudes continental regions (Hastenrath, 1991). The Asian Monsoon Anticyclone (AMA) is centered around 30° N and extends from the Pacific to Eastern Africa, with periodic elongations and filaments reaching the Atlantic coast of Africa. On its southern edge, the AMA is bounded by the Tropical Easterly Jet (TEJ) blowing over Africa from the Indian Ocean between 5 and 15° N. Previously, Barret

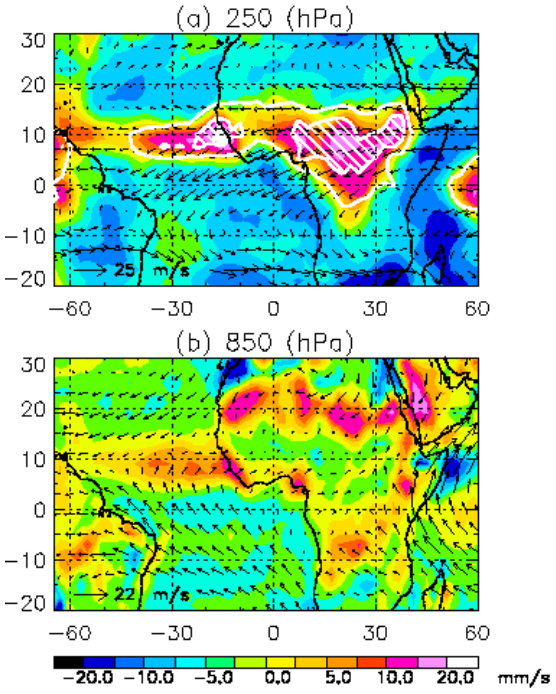

Fig. 1. August 2006 ECMWF winds. Black arrows represent horizontal winds and color contours vertical winds **(a)** 250 hPa **(b)** 850 hPa. White contours indicate deep convection (OLR contours 240 and 215 W/m^2, with values below 215 hatched white).

et al. (2008) have shown that variations in CO concentrations over Northern Africa at about 150 hPa are caused by elongations and filaments of the AMA and variations in the TEJ. The TEJ crosses the African ITCZ and subsequently diverges into a southeasterly flow over the Northern Atlantic and a strong northeasterly flow over the Gulf of Guinea and Southern Atlantic. These two anticyclonic UT systems recirculate the convective outflow from the ITCZ. From Central to Southern Africa, the upper branch of the winter Hadley cell is characterised by northerly winds changing from northeasterlies to northwesterlies resulting in a wind-shear region with near-zero zonal winds at ∼10° S (Fig. 1a).

5 Intercomparison of convective transport within the WAM region

In this section, we use the four different models to quantify the impact of African convective transport during the WAM upon the UT composition. We first inter-compare simulated convective mass fluxes that are directly related to the model parameterizations of convective transport. We then proceed to evaluate the modeled distributions of CO (which acts as a tracer for biomass burining) and O_3 (a product of the NO_x photochemistry) against satellite and airborne observations. The chemical lifetimes of these two species were computed for the JJA period in the tropical troposphere using the TM4

model. We found ∼1.2 months for CO and ∼4 days for O_3. This means that O_3 is a tracer for local transport such as convective uplift while CO can be transported far away from the active source region within the large scale Walker and Hadley cells. We performed a set of sensitivity studies defined for the purpose of differentiating the effects of convection and $LiNO_x$ parameterizations on the simulated distributions of CO and O_3. To examine the effect of $LiNO_x$ production (see Sect. 6) a sensitivity study was performed where the $LiNO_x$ production was switched off over a large box encompassing most of tropical Africa (between 30° S–20° N and 20° W–45° E, hereafter referred to as $LiNO_x$-off). A second sensitivity study was then defined where both $LiNO_x$ production and convective transport were switched off for an identical region (hereafter referred to as Conv-off). Both sensitivity simulations started on 1 June 2006. The effect of convective mixing examined in the present section is quantified as the difference between the $LiNO_x$-off and Conv-off simulations. Nevertheless, as mentioned by Lawrence and Salzmann (2008), in the tropics an important fraction of convective transport is occuring within the ascending branches of the large scale Hadley or Walker mean circulations. Part of the convective mass flux is therefore already accounted for by the large scale winds used to drive the advection schemes of the models. It implies that, even when parameterised convection is switched off, a large part of convective transport is still occuring in the simulations. This is especially true over central and West Africa during the monsoon that corresponds to an ascending branch of the Hadley cell. From our Conv-off simulations we therefore quantify the impact of parmeterised convective transport rather than real convective transport.

5.1 Analysis of convective mass fluxes

The analysis of the simulated FF distributions presented in Sect. 6 shows the differences between the models concerning the geographical location of the convective activity. We focus here on the vertical structure of convective transport based on Fig. 2 representing a latitude-pressure cross section of the detrainment and updraft mass fluxes averaged between 0–30° E. The latitudinal extension of convective activity from Fig. 2 is consistent with the FF shown in Fig. 11. MOCAGE convective activity exhibits maximum values around 5–15° N with a secondary maximum occuring just south of the equator, while TM4 simulates deep convection around 0–10° N. Previous studies with LMDz-INCA and MOCAGE have already compared the performance of different convective parameterizations. Josse et al. (2004) compared radon distributions simulated using both the Tiedtke and KFB schemes and found that the KFB scheme is more efficient in uplifting air from the free to the upper troposphere than the Tiedtke scheme, resulting in lower (resp. higher) radon concentrations in the free (resp. upper) troposphere. Similarly, based on simulations with the LMDz GCM, Hourdin et al. (2006) have shown that deep convection extends

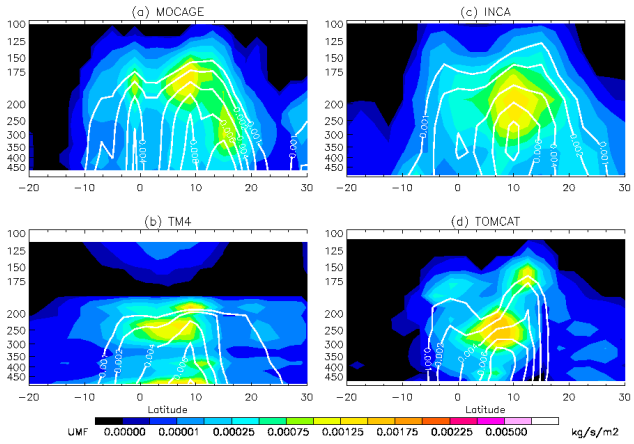

Fig. 2. August 2006 latitude-pressure cross-sections of convective mass fluxes averaged over 0° W–30° E from **(a)** MOCAGE **(b)** TM4 **(c)** INCA and **(d)** p-TOMCAT. Color contours represent the detrainment mass fluxes (kg/m^2/s) and solid white contours the updraft mas fluxes (0.001, 0.002, 0.004, 0.006, 0.008, 0.016 kg/m^2/s).

to higher altitudes with the Emanuel scheme than with the Tiedtke scheme. Comparisons between CO profiles simulated with LMDz-INCA also show that using versions of the Tiedtke scheme leads to more CO in the lower troposphere and less CO in the upper troposphere indicating a weaker convective transport than when using Emanuel scheme (Bouarar, PhD thesis). Williams et al. (2009a) have shown that the TM4 underestimation of UT O_3 relative to MOZAIC observations over Southern Africa during boreal summer is not related to soil nor biogenic emissions and they have suggested that it may be linked to a too weak convective uplift using the Tietdke scheme. The study of Tost et al. (2010) also corroborates our findings. Based on simulations with the ECHAM5/MESSy GCM, they examined the impact of convection parameterisation upon atmospheric chemistry modelling. In particular, comparing global mass fluxes, they show that the KFB scheme is responsible for deeper convective activity than the Tiedtke scheme, with "substantial mass fluxes up to 200 hPa and even higher". They further show that "an almost undiluted transport of CO-rich boundary layer air in the TTL" is responsible for higher concentrations of CO in the UT with the KFB scheme than with the other schemes. As outlined in Sect. 2 p-TOMCAT uses a modified version of the Tiedtke scheme where the entrainment and detrainment rates have been modified in order to bring convective clouds to higher altitudes. From this previous evidences, we can expect that convective transport will be weaker with TM4, than with p-TOMCAT, INCA and MOCAGE. This is confirmed by Fig. 2 where the convective mass fluxes are displayed for deep convection (above 500 hPa). The deep convective updrafts (0.001 kg/m^2/s upward mass flux contour) reach 125 hPa for INCA, 150 hPa for MOCAGE, 170 hPa for p-TOMCAT and only 200 hPa for

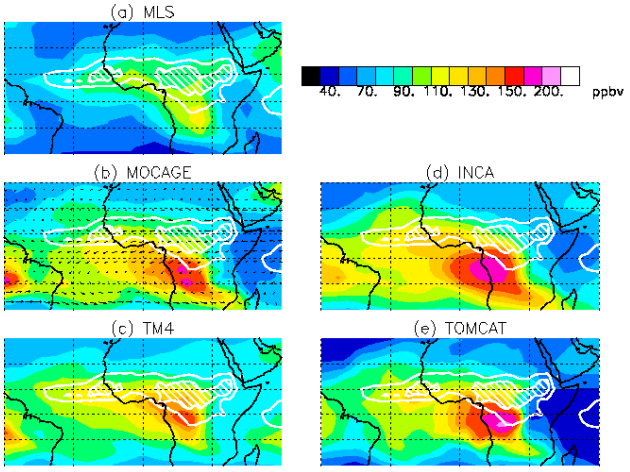

Fig. 3. August 2006 CO distribution at 215 hPa **(a)** Aura/MLS observations and simulations by **(b)** MOCAGE **(c)** TM4 **(d)** INCA and **(e)** p-TOMCAT. White contours indicate deep convection (OLR contours 240 and 215 W/m^2, with values below 215 hatched white).

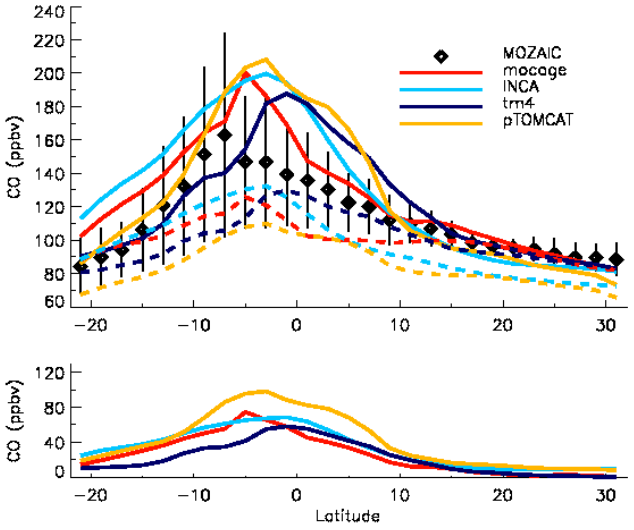

Fig. 4. August 2006 CO UT African transects. Upper panel: (diamonds) MOZAIC observations with error bars representing the variability (red) MOCAGE (light blue) INCA (dark blue) TM4 and (orange) p-TOMCAT (solid lines) L3JRCv2 inventory (dashed lines) GFEDv2 inventory. Lower panel: differences between simulations with the L3JRCv2 and the GFEDv2 inventory.

TM4. The 4 models detrain roughly between 2° S and 15° N with some important differences concerning the maxima of detrainment fluxes (see Fig. 2).

5.2 Impact on the CO distribution in the WAM upper troposphere

During the WAM, the primary source of CO in tropical Africa is BB from Southern Africa, which occurs south of the equator. Moreover, the relatively long atmospheric lifetime (∼1.2 months) means that the tropospheric distribution of CO allows one to evaluate the representation of the transport pathways from the BB region to the UT. Figure 3 compares the CO distributions at 215 hPa for August 2006 measured by MLS with those simulated by the 4 participating models. In Fig. 4 we show a similar comparison against the in-flight MOZAIC data, where the model means are calculated using interpolated model output to provide a coherent comparison. MLS fields show a CO maximum of ∼120 ppbv over Africa located between 0–10° S, whereas the CO maximum measured by MOZAIC reaches ∼160 ppbv at 7° S. MLS is therefore biased low by about 40 ppbv relative to MOZAIC. Nevertheless, the features from the MLS distribution (cf. Fig. 3a) give a good indication of the transport of the CO uplifted in the African UT. This transport is qualitatively characterized by southward transport within the upper branch of the southern predominant Hadley cell and accumulation in the wind-shear region (see Sect. 4), corresponding to where the maximum CO is measured by MLS. Westward transport by the TEJ occurs over the Atlantic, where again high concentrations of CO are measured. The CO distributions from the four models generally overestimate the distributions observed by MLS, with MOCAGE, INCA and p-TOMCAT maxima reaching ∼200 ppbv, whilst TM4 simulates values below 160 ppbv. The simulated continental maxima are located northwards from the MOZAIC maxima by 2° (MOCAGE), 4° (INCA and p-TOMCAT) and 6° (TM4). Nevertheless, MOCAGE, INCA and p-TOMCAT simulations lead to an overestimation in the CO maxima by up to ∼40 ppbv relative to MOZAIC and overestimate the outflow over the Gulf of Guinea relative to MLS. The values of the CO maxima simulated by TM4 are in slightly better agreement with MOZAIC observations (overestimation of ∼20 ppbv) and the distributions simulated with this model, particularly concerning the outflow over the Gulf of Guinea are closer to MLS values. Nevertheless, it has to be kept in mind that MLS CO concentrations may be biased low by up to 40 ppbv and are useful to characterize the large scale features of the CO UT distribution rather than to give absolute values.

To summarize, CO detrained by the Tietdke scheme from TM4 around 250 hPa is ascending slowly with the large scale vertical winds to the MOZAIC and MLS levels. This is resulting in a rather low CO maxima located within the ITCZ, in spite of the high CO emission flux in the L3JRCv2 emission inventory. With MOCAGE, INCA and p-TOMCAT, CO from BB is quickly uplifted by convection to levels higher than 200 hPa, where it is advected by the upper branch of the southern Hadley cell and accumulates within the wind-shear region (see Fig. 1a). These three models therefore simulate higher maxima south of the ITCZ. The CO maximum in the African UT simulated by INCA is broader than that

simulated by MOCAGE as a result of detrainment within a larger meridional region. South of the equator, MOCAGE and p-TOMCAT detrain at similar altitudes resulting in similar CO distributions south of the ITCZ. Between 0 and 10° N, the convective fluxes simulated by p-TOMCAT are much closer to those of TM4 resulting in comparable CO distributions north of the equator.

These results are in qualitative agreement with those from Williams et al. (2009b) who inter-compared the transport of passive tracers from the four AMMA models. The behavior of simulated CO described here is similar to the behavior of their Southern African tracer, whose latitude pressure cross-sections show maxima at ∼200 hPa and ∼5° S for MOCAGE and INCA and at ∼300 hPa and ∼0° S for TM4 and p-TOMCAT (using the previous version of the Tiedtke scheme with lower cloud tops). Additional simulations, in which the monthly GFEDv2 BB inventory was used (Fig. 4) for Africa, give CO concentrations lower by up to 100 ppbv around the latitudinal maximum but keep the locations of the maxima unchanged. Thus the GFEDv2 BB inventory leads to a strong undersestimation of the CO latitudinal maximum relative to MOZAIC for the participating models, which has also been identified in other studies Williams et al. (2010). From this analysis of both the simulated and observed CO distributions, we can conclude that for 2006 the appropriate CO emissions from African BB in boreal summer lie within the range of values provided by the GFEDv2 and the L3JRCv2 inventories and that part of the detrainment from convection from the WAM occurs above 200 hPa.

We now assess the impact of parameterised convective transport on the simulated CO distributions in the UT through the difference between the $LiNO_x$-off and Conv-off simulations (with $LiNO_x$ and both convective transport and $LiNO_x$ switched off over Africa, respectively). As emissions are identical in all the models and enhanced CO is analogous to a tracer of BB emissions from Southern Africa, the most important differences in simulated CO distributions are likely resulting from differences in the convection parameterizations. Figure 6 displays the differences in CO between the $LiNO_x$-off and Conv-off simulations at 250 hPa and Fig. 7 shows the latitude-pressure cross sections of the CO differences averaged over 0–30° E. In agreement with the CO budget established by Barret et al. (2008) a comparison of Fig. 6 and Fig. 3 clearly shows that the African distribution of CO around 200 hPa is mostly impacted by regional emission sources, subsequently uplifted by strong convection. Therefore, the model differences mostly result from differences in the convective transport representations. At 250 hPa, convective transport is responsible for CO enhancements ranging from 50 to 100 ppbv located over the western part of Africa within 0–15° S. The highest enhancements in CO are simulated by MOCAGE in the wind-shear region (around 10° S) described in Sect. 4 and by p-TOMCAT just south of the equator. With MOCAGE, INCA, and p-TOMCAT, convective CO enhancements are more important than with TM4 as a result of deeper convective transport as discussed in Sect. 5.1. In particular, MOCAGE, INCA and p-TOMCAT simulate convective CO enhancements of more than 40 ppbv extending southeastward to the Gulf of Mozambique following the southern anticyclonic circulation described in Sect. 4. The latitude pressure cross-sections of the CO differences computed for the 0°–30° E zone further highlight the model differences. The different models display the same general dipolar structure with a CO depletion in the lower-mid troposphere from ∼10° S to ∼20° N and a CO enrichment in the UT south of the equator. The main differences concern the altitude dependence of the differences in good agreement with the 50 to 100 hPa downwards shift of the deep convection detrainment of TM4 relative to the other models as discussed in Sect. 5.1 (see Fig. 2). As already mentioned, our approach allows us to quantify the impact of parameterised convective transport rather than real convective transport on the CO distributions. We discuss here the possible artefacts implied by this approach. Convection above central Africa, north of the equator, is associated with the monsoon and the large scale Hadley circulation. On the contrary, above south-central Africa convection which is less important (Fig. 1) is probably linked to local MCS but not to the large scale mean circulation. Consequently, the impact of real convective transport is probably underestimated north of the equator and convection may be responsible for a less pronounced CO latitudinal gradient that what is displayed in Fig. 6 and Fig. 7.

5.3 Impact on the O_3 distribution in the WAM troposphere

Before quantifying the impact of convection upon the UT O_3, we present an evaluation of the simulated distributions through comparison with observations. Distributions of O_3 at 215 hPa simulated by the participating models and observed by MLS are displayed in Fig. 8. The African UT O_3 transects from model simulations and MOZAIC observations are shown in Fig. 5. Both MLS and MOZAIC show similar features concerning the distribution of O_3 over Africa. The highest values occur between 5–20° S, where there is a negative gradient towards the minimum centered around the ITCZ and a positive gradient towards the north. The latitudinal O_3 minima observed from MLS closely follows the ITCZ contour from Eastern Africa towards the Atlantic. The models roughly capture the latitudinal behavior from the observations although there are some important differences. For instance, MOCAGE overestimates O_3 relative to MOZAIC over the whole latitudinal transect by less than 5 ppbv south of 8° S and by about 15 ppbv north of the equator. The elevated O_3 concentrations simulated by MOCAGE north of 10° N are probably partly caused by the strong Stratosphere-To-Troposphere Exchange (STE) simulated by this model in this region as shown in Williams et al. (2009b). In contrast, the 3 other models underestimate O_3 south of the equator by up to 20 ppbv for INCA and less than 10 ppbv (within

Table 2. Simulated total FF and $LiNO_x$ production over Africa (20° S–30° N and 20° W–40° E).

Variable	Model MOCAGE	TM4	INCA	p-TOMCAT	Observation LIS
FF (s^{-1})	2.9	5.5	8.9	6.2	12.3
$LiNO_x$ (Tg N)	0.039	0.077	0.12	0.15	

the monthly variability measured by MOZAIC) for TM4 and p-TOMCAT. Moreover, the agreement is quite good with MOZAIC north of 10° N for INCA and TM4. These biases are consistent with comparisons of the simulated distributions versus the MLS observations at 215 hPa. In particular, MOCAGE shows a better agreement with MLS over Southern Africa and the Southern Atlantic than the other models that are underestimating O_3 in this region. The differences in the $LiNO_x$ production are not likely to explain the differences in O_3 (see Sect. 6). Indeed, although MOCAGE has the lowest $LiNO_x$ production (see Table 2) UT O_3 concentrations are higher than in any of the other models. However, the discussion of Sect. 6 shows that the major impact of $LiNO_x$ occurs above the ocean rather than above the continent. The run with the GFEDv2 inventory for African BB (Fig. 5) helps to understand the differences between the models. The UT O_3 differences between the L3JRCv2 and GFEDv2 runs are maxima between 10° S and 5° N with differences reaching 15 ppbv for MOCAGE, 8 ppbv for INCA and ∼5 ppbv for TM4 and p-TOMCAT. Consistently with the previous discussion about CO, the higher altitude of the convective detrainment explains the stronger impact of the African BB inventory at the MOZAIC altitudes upon UT O_3 with MOCAGE than with TM4. The reason for the difference between MOCAGE and the other models regarding UT O_3 is probably related to the chemistry scheme. This is discussed in detail by Ordóñez et al. (2010) in their study about multi-model simulations of air pollution over Europe. They have shown that the MOCAGE tropospheric chemistry scheme (RACM) was producing excessive O_3 in the lower-mid troposphere at midlatitudes. For the 4 models, the maxima of O_3 produced by Southern African BB (not shown) are located at ∼800 hPa between roughly 12 and 2° S. MOCAGE produces excessive O_3 in the BB region with maxima at 800 hPa reaching 200 ppbv compared to 100–150 ppbv for the other models. It has to be noted that the lowest O_3 concentrations in the BB region are simulated by INCA (not shown). This difference is of the same order as the difference between MOCAGE and TM5 or MOZART reported in Ordóñez et al. (2010) concerning surface O_3 over Europe during summer 2003. With MOCAGE, the uplift of the excess of O_3 produced from BB in the Southern African lower troposphere follows the same pathway as CO and accumulates in the wind-shear region resulting in an excess of O_3 relative to the other models. The 3 other models underestimate O_3 concentrations relative to

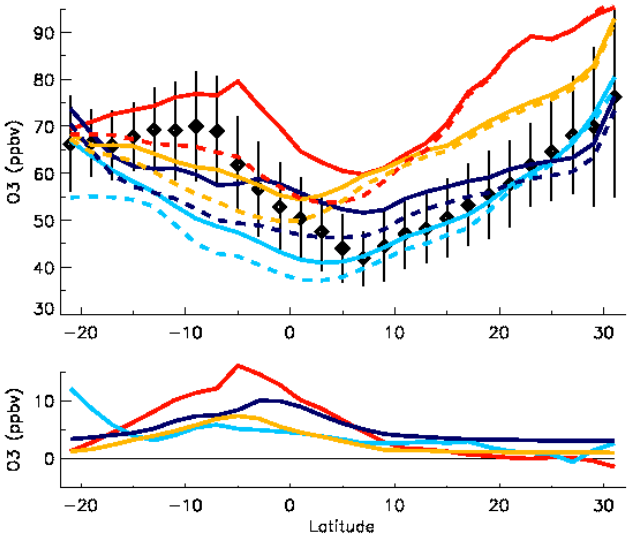

Fig. 5. Same as Fig. 4 but for O_3.

MOZAIC or MLS in this region (around 10° S). Their O_3 production from the African BB maybe underestimated.

The impact of tropical deep convection upon tropospheric O_3 has been studied by Lawrence et al. (2003). They have shown that over clean regions, convective mixing reduces the tropospheric O_3 lifetime through the uplift of O_3 poor air masses from the surface (where the O_3 lifetime is low) to the UT (where the O_3 lifetime is high) and simultaneous compensatory subsidence of O_3 rich air masses downwards from the UT to the lower troposphere. According to their study convective mixing over polluted regions leads to slightly increase the chemical lifetime of tropospheric O_3 and to inject chemical O_3 precursors emitted at the surface in the outflow of large convective systems where their chemical lifetime is longer and therefore to enhance the O_3 photochemical production. From simulations with the MATCH-MPIC model, they find that convection results in an increase of the global tropospheric O_3 burden. In contrast, the study of Doherty et al. (2005) based on simulations from the STOCHEM-HadAM3 model, shows that the O_3 lifetime changes related to deep convection result in a reduction of the tropospheric O_3 burden. While Lawrence et al. (2003) and Doherty et al. (2005) quantified the impact of convection upon tropospheric O_3 on the annual and global scales, our study is focused upon

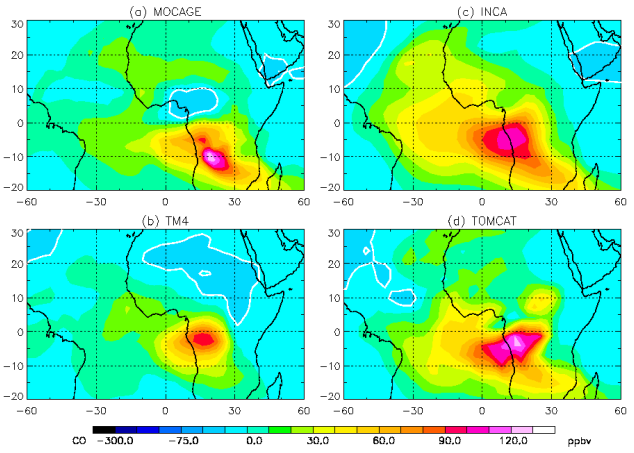

Fig. 6. August 2006 distributions of 250 hPa CO difference between $LiNO_x$-off and Conv-off simulations by **(a)** MOCAGE **(b)** TM4 **(c)** INCA and **(d)** p-TOMCAT.

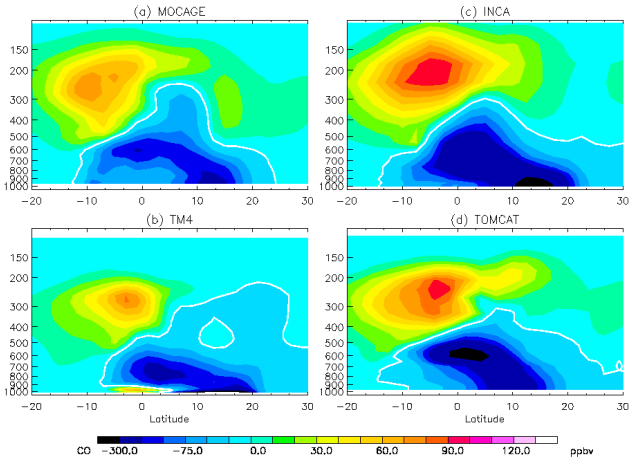

Fig. 7. August 2006 latitude-pressure cross-sections averaged over 0°–30° E of CO difference between $LiNO_x$-off and Conv-off simulations by **(a)** MOCAGE **(b)** TM4 **(c)** INCA and **(d)** p-TOMCAT.

the WAM at the African scale. Furthermore, performing simulations with similar emission inventories, our goal is to explain the possible causes for differences among the four models involved in the AMMA project concerning the impact of convection on tropospheric O_3.

The differences in O_3 between the $LiNO_x$-off and Conv-off simulations at 250 hPa are shown in Fig. 9 with the latitude-pressure cross sections of the differences averaged over 0–30° E being shown in Fig. 10. For all the models, the UT convective O_3 depletion extends from the continental ITCZ to the Northern Atlantic as a result of transport by the northern anticyclonic circulation (Sect. 4). The models simulate convective O_3 enhancements over Africa south of the equator. These O_3 enhancements are consistently collocated with the CO convective enhancements from Fig. 6 discussed previously, clearly indicating a BB origin for this O_3. Nevertheless, the models are not in quantitative agreement concerning this O_3 convective enhancement. More particularly, the O_3 convective increase at 250 hPa around 10° S is much higher for MOCAGE than for the other models. South of 5° N the latitude-pressure cross-sections of the $LiNO_x$-off and Conv-off differences (Fig. 10) are in qualitative agreement for the four models and show features similar to those of the CO cross-sections (Fig. 7). The main comparable feature between CO and O_3 cross-sections is the dipolar structure with depletion in the lower-mid troposphere and increase in the upper troposphere. As previously discussed, the consistency between O_3 and CO enhancements is a clear signature of BB. The O_3 increase is stronger for MOCAGE (20 ppbv) than for p-TOMCAT and INCA (12.5 ppbv) while it was the opposite concerning CO. This clearly indicates an excessive O_3 production from BB precursors in MOCAGE and probably an insufficient production in INCA and in p-TOMCAT to a lesser extent, which both simulate low O_3 concentrations in the BB region. As already discussed, this is in agreement with the intercomparison study by Ordóñez et al. (2010) which shows that the MOCAGE tropospheric scheme is producing excessive O_3 in the lower-mid troposphere at midlatitudes. Nevertheless, as was mentioned previously, MOCAGE is the only model able to reproduce the shape of the O_3 transect south of the equator with a slow increase south of 5° S and a sharp decrease north of 7° S. The O_3 from the other models is continuously decreasing northwards to the equator and is underestimated relative to the MOZAIC and MLS measurements. As a result of weaker convective transport, the O_3 dipole is not so pronounced for TM4 as it is for the other models.

6 Impact of the $LiNO_x$ source in the WAM region

Martin et al. (2002) and Sauvage et al. (2007c) have quantified the seasonal variability of the impact of the global $LiNO_x$ source upon tropospheric O_3 using sensitivity simulations with the GEOS-Chem CTM. They have established that $LiNO_x$ is the main source governing the Wave-1 pattern and the tropical Atlantic paradox. In the present study, we aim at making a detailed analysis of the impact of African $LiNO_x$ emissions during the WAM upon the tropical UT composition. The use of four different CTMs allows us to evaluate the error induced by inter-model differences concerning this impact. An evaluation of the lightning activity simulated by the four CTMs against spaceborne observations is first presented. We then proceed to analyse the effect of $LiNO_x$ production based on the differences between the Baseline simulations and the $LiNO_x$-off simulations described in Sect. 5. The NO concentrations from the models are then evaluated against airborne observations from the AMMA campaign.

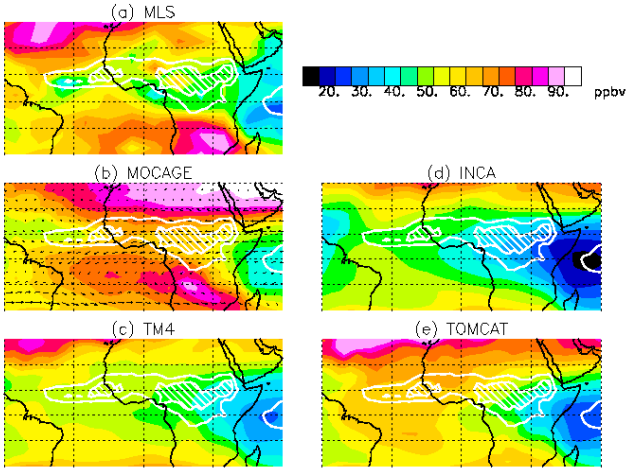

Fig. 8. August 2006 O_3 distribution at 215 hPa **(a)** Aura/MLS observations and simulations by **(b)** MOCAGE **(c)** TM4 **(d)** INCA and **(e)** p-TOMCAT. White contours indicate deep convection (OLR contours 240 and 215 W/m^2, with values below 215 hatched white).

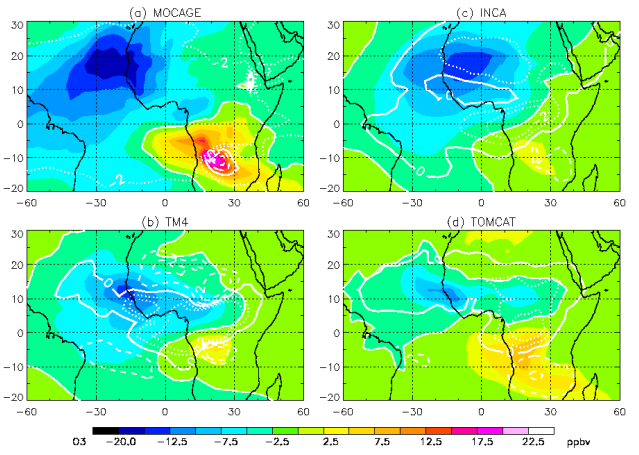

Fig. 9. August 2006 distributions of 250 hPa O_3 difference between $LiNO_x$-off and Conv-off simulations by **(a)** MOCAGE **(b)** TM4 **(c)** INCA and **(d)** p-TOMCAT. White contours represent the same differences but for tropospheric columns of O_3 with 1 DU intervals from −2 to 2 DU.

Our results are qualitatively compared to those presented by Martin et al. (2002) and Sauvage et al. (2007c).

6.1 Analysis of the lightning activity during summer over West Africa

Lightning parameterizations from the different models are based on the use of meteorological model parameters as proxies for the FF. MOCAGE, INCA and p-TOMCAT have all adopted the lightning parametrization from Price and Rind (1992) where the FF is related to the convective cloud top height (CTH). Based on climatological data, Price and Rind (1992) have shown that the FF is empirically related to $CTH^{4.9}$ over land surfaces and $CTH^{1.7}$ over the sea. This parametrization has important limitations such as the failure to reproduce land and sea contrasts in FF with a single law. The parametrization of Price and Rind (1992) tends to overestimate (resp. underestimate) the flash activity over South America (resp. Central Africa) in comparison to LIS observations, as is the case with the MATCH-MPIC CTM (Labrador et al., 2005). Other parameterizations have also been developed based on the relationship between the FF and other convection variables. For instance, TM4 uses a linear relationship between lightning flashes and convective precipitation, which gave the best correlation results for summer conditions over Europe (Meijer et al., 2001). In a comprehensive study, Tost et al. (2007) have made comparisons between various FF parameterizations based on CTH, convective precipitation, updraft velocity and updraft mass flux, combined with various convective transport parameterizations in the ECHAM/Messy GCM. Most of the combined parameterizations are not able to reproduce the right ratio between African and South American FF's, and underestimate or miss the maximum in FF that occurs over Central Africa.

In order to evaluate the FF distributions simulated by the four different models participating in this study, we use the observations from the Lightning Imaging Sensor (LIS) (Christian et al., 2003). Figure 11a displays the climatological FF for August over Africa based on 10 years of LIS data (1995–2005), and the total FF over Africa simulated by each of the models is given in Table 2. It can be clearly seen that the most intense lightning activity is located within the continental ITCZ represented by the OLR contours in Fig. 1. Large FF's are found from 10° S to about 18° N over Africa with the global maximum localised around the equator in Central Africa as shown already by Christian et al. (2003). The FF's simulated by each of the models, displayed in Fig. 11b–e, show differences in both the distribution and in the intensity of the lightning activity. MOCAGE FF's are low, but the geographical pattern of high FF's is somewhat similar to the LIS climatology. The FF's intensities simulated by TM4 are in relatively good agreement with the LIS climatology but the FF's over Southern Sahel are lower than measured by LIS. LMDz-INCA and p-TOMCAT simulate a range of FF's intensities similar to LIS but with values over the Sahel more intense than observed by LIS. This overestimation is a result of the deeper convective activity computed by these 2 models over Sahel than over Central Africa as can be seen in Fig. 2. The figures from Table 2 show that MOCAGE (resp. TM4 and p-TOMCAT) underestimates African lightning by a factor of ∼4 (resp. ∼2) while INCA gives a value relatively close to the LIS climatology. All the AMMA-MIP models underestimate the lightning maximum over Central Africa, similar to most of the combined parameterizations tested in Tost et al. (2007). A similar problem has

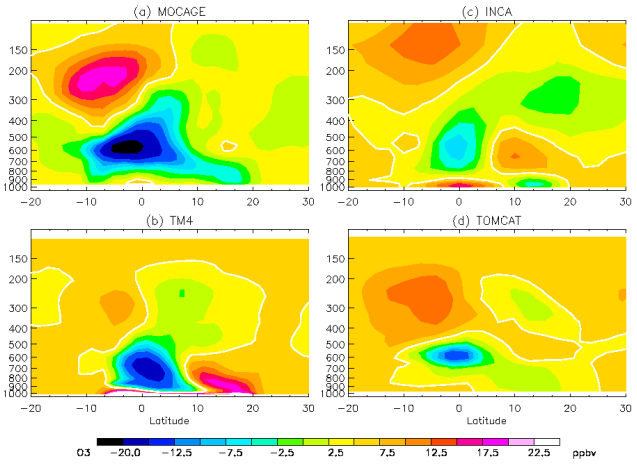

Fig. 10. August 2006 latitude-pressure cross-sections averaged over 0°–30° E of O_3 difference between $LiNO_x$-off and Conv-off simulations by **(a)** MOCAGE **(b)** TM4 **(c)** INCA and **(d)** p-TOMCAT.

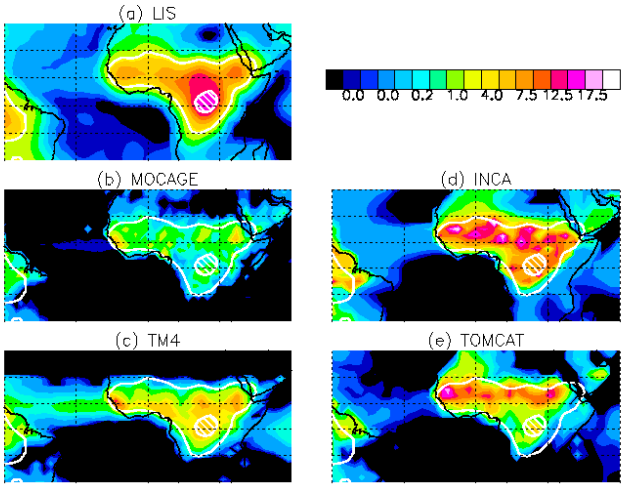

Fig. 11. August lightning flash frequencies in 100xflashes/km2/day **(a)** climatology from 10 years (1995–2005) LIS observations and simulations by **(b)** MOCAGE **(c)** TM4 **(d)** INCA and **(e)** p-TOMCAT. White contours indicate lightning flash frequencies of 0.04 and 0.15 flashes/km^2/day as observed by LIS, with values above 0.15 hatched white.

already been reported by Jourdain and Hauglustaine (2001) for LMDz-INCA. One should note that most models normalise the flash rates by a global scaling factor to obtain a fixed total NO_x production by lightning.

6.2 Impact on the NO_x distribution in the upper troposphere

As mentioned in Sect. 2 the total amount of $LiNO_x$ produced by the models range from 3–5 TgN/yr. Table 2 shows that TM4, INCA, and p-TOMCAT produce, respectively 2–4 times more $LiNO_x$ over Africa during August 2006 than MOCAGE. The values given in Table 2 show that the amount of $LiNO_x$ produced by the models over Africa closely follows the integrated African FF despite some differences between the models concerning the computations of the IC/CG ratios or the number of NO_x molecules produced per flash. The distributions of LiNOX has been computed as the difference between the Baseline runs and the $LiNO_x$-off simulations. The UT $LiNO_x$ distributions (not shown) from the different models closely follow the FF distributions (Fig. 11). In particular MOCAGE simulates low $LiNO_x$ amounts with maxima corresponding to locations with highest FF's (see Sect. 5). INCA and p-TOMCAT (resp. TM4) produce more homogeneous $LiNO_x$ distributions with maxima between 10–20° N (resp. 5–15° N).

The latitude-pressure cross-sections of $LiNO_x$ for the 30° W–30° E zone (Fig. 12) show important differences between the models. The $LiNO_x$ zonal maximum from TM4 (∼140 pptv) is simulated between 200–300 hPa around 10° N. This is in agreement with the $LiNO_x$ vertical placement prescribed according to Pickering et al. (1998) with most of the NO_x injected between the −15° isotherm and the cloud top (below 200 hPa in TM4 according to Fig. 2). MOCAGE $LiNO_x$ mixing ratios maxima are lower (100 pptv) but located at higher altitude (between 120 and 200 hPa) and at almost the same latitude as TM4. In MOCAGE, no vertical placement is prescribed and the NO_x emitted within the cloud are transported according to the convective mass fluxes (Mari et al., 2006). The zonal $LiNO_x$ maximum (Fig. 12) is therefore roughly collocated with the maximum of cloud detrainment (Fig. 2). $LiNO_x$ from INCA reach values of 140 pptv and are distributed from 100 down to 400 hPa between 10 and 20° N. This is in agreement with the use of the profile of $LiNO_x$ mass distribution from Pickering et al. (1998) rescaled with the modeled CTH. As we have already discussed, convection is deeper with the Emanuel scheme compared to the Tiedtke scheme from TM4 leading to $LiNO_x$ reaching higher altitudes in INCA than in TM4. Finally, $LiNO_x$ produced by p-TOMCAT are mostly distributed between 10–20° N and between 200–300 hPa and reach higher values (400 pptv) than either INCA or TM4 in line with the values given in Table 2.

The NO observations obtained during AMMA by the Falcon 20 from the DLR allows us to partially validate the $LiNO_x$ produced by the different models in the observation region around Ouagadougou (12.4° N and 1.5° W). Figure 13 displays the observed and modeled NO mean profiles correponding to air masses that have been impacted by convection (CONV) and air masses that have not been impacted by convection (NOCONV). Concerning the observations, the differences are very important between 200–350 hPa with NOCONV NO mean concentrations ranging from 100–200 pptv while mean NO concentrations range from 250 pptv (350 hPa) to 500 pptv (180 hPa) in the CONV

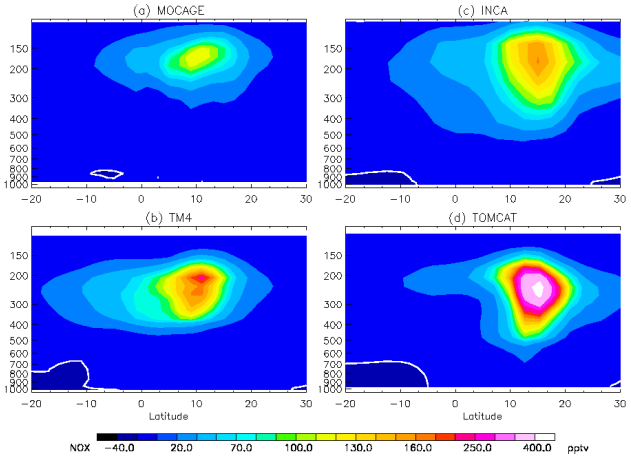

Fig. 12. August 2006 $LiNO_x$ latitude-pressure cross-sections averaged over 30° W–30° E computed as the difference between Baseline and $LiNO_x$-off simulations by **(a)** MOCAGE **(b)** TM4 **(c)** INCA and **(d)** p-TOMCAT.

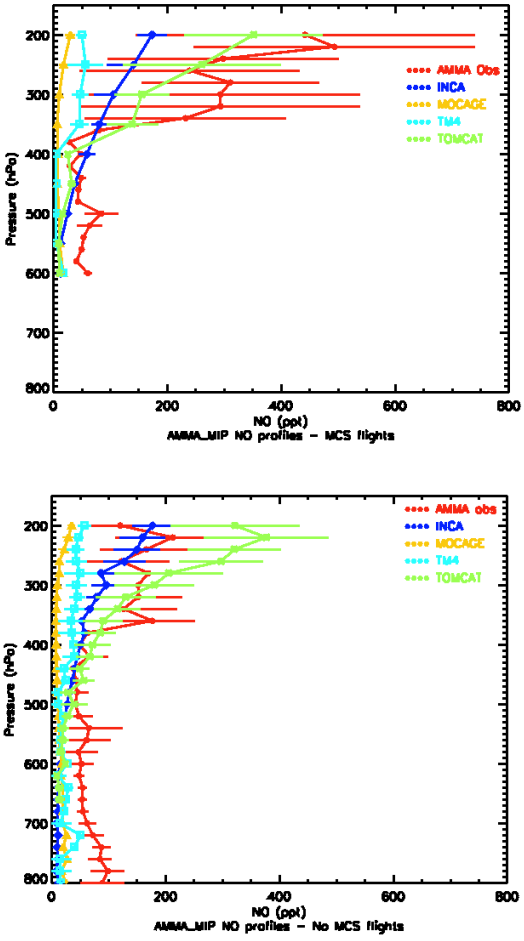

Fig. 13. Vertical profiles of NO mixing ratios observed during the AMMA campaign in August 2006 by the DLR Falcon 20 and simulated by the MOCAGE, INCA, TM4 and p-TOMCAT CTM's. (top) observations that have been impacted by deep convection in the previous 3–4 days (CONV cases) (bottom) observations that have not been impacted by deep convection (NOCONV cases).

case. Conversely, the correponding NO concentrations simulated by the different models show little differences between the CONV and NOCONV cases. This is not surprising because the models are not enable to represent convective systems even as large as MCS whose sizes are comparable to the size of the model gridboxes. On the other hand, there are large differences between the models concerning NO concentrations in the UT clearly related to the $LiNO_x$ production. The UT NO concentrations simulated by the models follow the figures of integrated NO_x production from Table 2. p-TOMCAT simulates the highest NO concentrations comparable to the CONV observations and NO concentrations from INCA are in good agreement with the NOCONV observations between 200–300 hPa. The high electrical activity simulated by p-TOMCAT and INCA in the region around Ouagadougou where the DLR Falcon observations were carried out (see Fig. 11) is therefore realistic. Both TM4 and MOCAGE simulate much lower UT NO concentrations than observed with, respectively ∼100 and ∼50 pptv. The low NO concentrations simulated by TM4 and MOCAGE are a result of the low electric activity that these 2 models reproduce over the part of West Africa sampled by the DLR Falcon (see Fig. 11). Furthermore as discussed below, MOCAGE $LiNO_x$ are maxima above 200, the highest altitude reached by the DLR Falcon.

6.3 Impact on the O_3 distribution in the upper troposphere

The differences in UT (250 hPa) O_3 between the Baseline and $LiNO_x$-off simulations are displayed in Fig. 14. Here it can be seen that $LiNO_x$ over Africa is principally impacting O_3 over the Atlantic Ocean following the transport of the ITCZ outflow by the TEJ and the northern and southern anticyclonic circulations (see Sect. 4). The region exhibiting the largest effect is the northern tropical Atlantic between the West African coast and 45° W. Here, maxima in O_3 enhancements vary between about 10 ppbv (MOCAGE) to more than 20 ppbv (INCA). Following the distribution of Lightning activity (Fig. 11), the O_3 enhancement is stronger (resp. weaker) north of 10° N with INCA and p-TOMCAT (resp. TM4). The impact over Africa is substantially lower than over Northern Atlantic and is decreasing eastwards. At 15° W, from Southern to Northern Africa, the O_3 enhancements are within 2.5–5 ppbv for MOCAGE and 2.5–10 ppbv for the other models. The maxima continental enhancements are simulated over Southern Africa and extend to Madagascar following transport of LiNOX-impacted air masses by the southwesterly anticyclonic flow (Fig. 1).

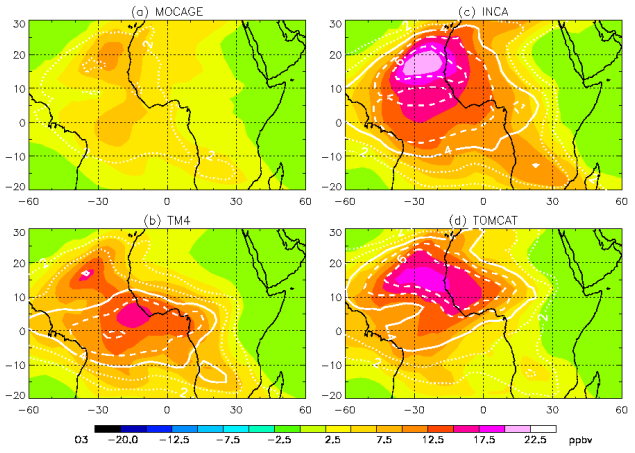

Fig. 14. August 2006 distributions of 250 hPa O_3 difference between Baseline and $LiNO_x$-off simulations by **(a)** MOCAGE **(b)** TM4 **(c)** INCA and **(d)** p-TOMCAT. White contours represent the same differences but for tropospheric columns of O_3 with 1 DU intervals from 2 to 6 DU.

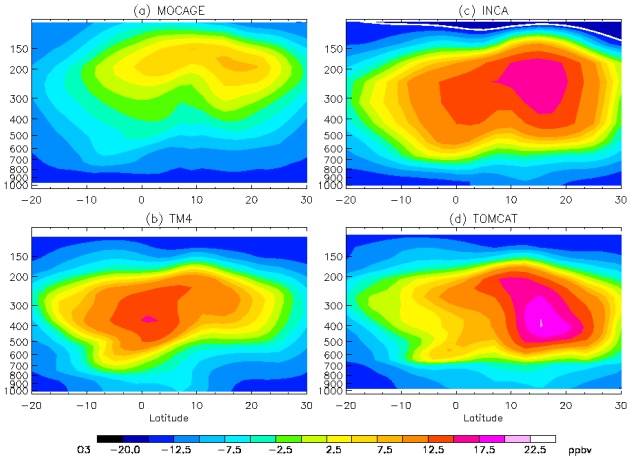

Fig. 15. August 2006 latitude-pressure cross-sections averaged over 45° W–0° E of O_3 difference between Baseline and $LiNO_x$-off simulations by **(a)** MOCAGE **(b)** TM4 **(c)** INCA and **(d)** p-TOMCAT.

The tropospheric O_3 column enhancements from lightning emissions for JJA from Martin et al. (2002) and Sauvage et al. (2007c) are comparable. The highest enhancements (8 to 12 DU) are simulated over the tropical Atlantic between 10° S and 10° N. If we assume, as suggested by Jenkins and Ryu (2004) that the most important $LiNO_x$ source contributing to this tropical Atlantic enhancement is Africa, we can make a rough estimate of the African contribution by substracting the enhancement over the remote Pacific (6 DU for Martin et al. (2002) and 5 DU for Sauvage et al. (2007c)) from the South Atlantic enhancement. We find that African $LiNO_x$ contribute to 4 (resp. 6) DU to the O_3 tropospheric column enhancement over the tropical Atlantic in Martin et al. (2002) (resp. Sauvage et al., 2007c). In order to make a qualitative comparison, we computed O_3 tropospheric column enhancements from the AMMA CTM's (see Fig. 14). For TM4, INCA and p-TOMCAT, the maxima (5 to 7 DU) agree with Martin et al. (2002) and Sauvage et al. (2007c). MOCAGE is strongly underestimating the $LiNO_x$ impact upon the tropical Atlantic O_3 tropospheric columns (2 DU) relative to the other models because it is producing less $LiNO_x$ and because $LiNO_x$ are injected too high in the troposphere. The participating models simulate important tropospheric column enhancements over the tropical Atlantic between 10 and 20° N which are not present in Martin et al. (2002) and Sauvage et al. (2007c). The difference can be partly explained by the fact that Martin et al. (2002) and Sauvage et al. (2007c) are showing averages over the whole JJA season and we are analysing the month of August only. In June, the ITCZ is about 5° S more to the south compared to August resulting in a southwards shift of both lightning and convective outflow. The most important difference between INCA and both TM4 and the estimate of Martin et al. (2002) and Sauvage et al. (2007c) is that INCA simulates the maximum O_3 enhancement (7 DU) over the tropical Atlantic between 10 and 20° N. The same is true for p-TOMCAT. This is clearly a result of the elevated FF's simulated by INCA and p-TOMCAT at the northern edge of the ITCZ, which are overestimated according to the LIS observations (see Fig. 11). The absence of any enhancement simulated with the model used by Sauvage et al. (2007c), where the spatial distribution of lightning is scaled to spaceborne observations, further indicates the likely overestimation of this feature by INCA and p-TOMCAT. Nevertheless, the good agreement between NO airborne observations by the DLR Falcon 20 and INCA and p-TOMCAT simulations around Ouagadougou clearly mitigate this statement.

The differences in tropospheric O_3 between the baseline and the $LiNO_x$-off simulations are shown in Fig. 15 as averaged between longitudes 0–45° W (where the $LiNO_x$ have the highest impact upon O_3). As for NO_x (Fig. 12) MOCAGE simulates O_3 zonal enhancement to be less intense and located at higher altitudes (120–300 hPa) than the other models. The models in which the most important impact occurs are INCA and p-TOMCAT, with values exceeding 15 ppbv between 200–500 hPa and 10–20° N. As a result of the difference in the geographical distribution of $LiNO_x$ (Fig. 12), zonal enhancements in TM4 are somewhat comparable to INCA south of 10° N but are much lower northwards. O_3 production from $LiNO_x$ is lower in p-TOMCAT than in TM4 and INCA south of 10° N because of the lower FF simulated in this region by p-TOMCAT (see Fig. 11).

7 Conclusions

In this study we have evaluated the impact of convective mixing and $LiNO_x$ from Africa during the 2006 WAM using the four different state-of-the-art 3-D global chemistry transport models which are involved in the AMMA-MIP project. The different models reproduce qualitatively the CO and O_3 distributions observed by the MOZAIC airborne program or Aura/MLS spaceborne observations over Africa and the tropical Atlantic, albeit with some important differences.

Concerning CO in the African UT, which can be considered as a tracer from Southern African BB, the most important inter-model differences involve the position of the latitudinal CO maximum. MOCAGE simulates the CO latitudinal maxima around ∼5° S in good agreement with the MOZAIC observations. The maxima simulated by INCA and p-TOMCAT are located further 2° northwards and TM4 CO maximum is located about 6° to the north relative to the MOZAIC maximum. All the models generally overestimate the CO maxima by 20 to 40 ppbv relative to the MOZAIC measurements indicating a probable overestimation of CO emissions from South African BB in the L3JRC inventory. The intercomparison of the convective mass fluxes from the different models highlighted the determining influence of convective parameterizations upon the distributions of CO in the UT. The maximum detrainment from African deep convection during the monsoon simulated by MOCAGE, INCA and p-TOMCAT (resp. TM4) occurs partly above 200 hPa (resp. 300 hPa). Therefore, CO enriched air masses detrained within the upper branch of the Hadley winter cell accumulate in the zonal wind-shear region around 5° S where the CO maximum concentration is observed by MOZAIC. With TM4, the detrained air masses ascend more slowly to the altitude of maximum meridional winds from the Hadley cell and the CO concentrations are maxima within the ITCZ.

Over Africa, the modeled and observed O_3 distributions along a latitudinal transect are roughly characterized by high values south of the ITCZ, low values within the ITCZ and again high values north of the ITCZ. Three models out of 4 (INCA, TM4 and p-TOMCAT) underestimate the O_3 concentrations around 10° S by ∼10–20 ppbv. MOCAGE overestimates the O_3 concentrations by 5–15 ppbv relative to the MOZAIC observations but better represents the shape of the O_3 African transect south of the equator. The collocation of CO and O_3 elevated values and evidences from sensitivity simulations with convective mixing switched off clearly indicate the impact of Southern African BB upon the composition of the UT south of the ITCZ. In the case of O_3, the differences between models can partly be attributed to differences in convective transport parameterizations but are mostly due to differences in the efficiency of photochemical production of O_3 in the BB region. MOCAGE (resp. INCA) produces the highest (resp. the lowest) O_3 concentrations in the lower troposphere within the fire region with concentrations reaching 200 ppbv (resp. 100 ppbv). Therefore, INCA cannot reproduce the elevated O_3 concentrations collocated with the CO maxima as it is the case with MOCAGE.

The influence of $LiNO_x$ upon O_3 in the African UT has also been evaluated with sensitivity simulations from the AMMA models. Our results confirm that the contribution of African $LiNO_x$ is the most important over the tropical Atlantic. The $LiNO_x$ contribution to the UT African latitudinal gradient (∼20° E) is lower (∼5 ppbv) than the impact of convective mixing (∼10 ppbv). The most important O_3 enhancements from $LiNO_x$ are simulated over the tropical Atlantic, north (resp. south) of 10° N with INCA and p-TOMCAT (resp. TM4). Comparisons between modeled and observed FF's points out that TM4 FF's are in good agreement both in intensity and location with LIS south of 10° N but too low northwards while INCA and p-TOMCAT simulate too elevated FF's over the Sahel north of 15° N. AMMA airborne observations have shown that none of the models are able to reproduce the impact of individual MCS on the NO UT concentrations, but that p-TOMCAT and INCA best reproduce the elevated NO concentrations observed just south of the Sahel while MOCAGE and TM4 largely underestimate them. We can therefore estimate that $LiNO_x$ emitted from Africa during the month of August 2006 range within 0.08–0.15 TgN and that their impact upon tropospheric O_3 is mostly important over the tropical Atlantic between 10° S and 20° N.

Acknowledgements. Based on a French initiative, AMMA was built by an international scientific group and is currently funded by a large number of agencies, especially from France, the UK, the USA, and Africa. It has been the beneficiary of a major financial contribution from the European Community's Sixth Framework Research Programme. The authors acknowledge for the strong support of the European Commission, Airbus, and the Airlines (Austrian-Airlines, Austrian, Air France) who carry free of charge the MOZAIC equipment and perform the maintenance since 1994. MOZAIC is presently funded by INSU-CNRS, Meteo-France, and FZJ (Forschungszentrum Julich, Germany). Costs of transport for the MOZAIC instrumentation onboard the Air Namibia aircraft in 2006 were paid by INSU-CNRS and by the Network of Excellence ACCENT; maintenance costs were paid by FZJ. The Falcon NO measurements were co-funded by DLR within the Earth Observation Programme. We thank Michael Lichtenstern and Paul Stock of DLR for their help in acquiring this NO data set. The Aura/MLS data were kindly provided by the MLS team at NASA/JPL. Interpolated OLR data are provided by the NOAA/OAR/ESRL PSD, Boulder, Colorado, USA, from their web site at http://www.cdc.noaa.gov.

Edited by: C. Reeves

The publication of this article is financed by CNRS-INSU.

References

Barret, B., Ricaud, P., Mari, C., Attié, J.-L., Bousserez, N., Josse, B., Le Flochmoën, E., Livesey, N. J., Massart, S., Peuch, V.-H., Piacentini, A., Sauvage, B., Thouret, V., and Cammas, J.-P.: Transport pathways of CO in the African upper troposphere during the monsoon season: a study based upon the assimilation of spaceborne observations, Atmos. Chem. Phys., 8, 3231–3246, doi:10.5194/acp-8-3231-2008, 2008.

Bechtold, P., Bazile, E., Guichard, F., Mascart, P., and Richard, E.: A mass flux convection scheme for regional and global models, Q. J. Roy. Meteor. Soc., 127, 869–886, 2001.

Bernath, P. F., McElroy, C. T., Abrams, M. C., et al.: Atmospheric Chemistry Experiment (ACE): mission overview, Geophys. Res. Lett., 32, L15S01, doi:doi:10.1029/2005GL022386, 2005.

Bian, H., Chin, M., Kawa, S. R., Duncan, B., Arellano, A., and Kasibharla, P.: Sensitivity of global CO simulations to uncertainties in biomass burning sources, J. Geophys. Res., 112, D23308, doi:10.1029/2006JD008376, 2007.

Bond, D. W., Steiger, S., Zhang, R. Y., et al.: The importance of NO_x production by lightning in the tropics, Atmos. Environ., 36, 1509–1519, 2002.

Bousserez, N., Attie, J.-L., Peuch, V.-H., et al.: Evaluation of the MOCAGE chemistry transport model during the ICARTT/ITOP experiment, J. Geophys. Res., 112, D10S42, doi:10.1029/2006JD007595, 2007.

Carver, G. D., Brown, P. D., and Wild, O.: The ASAD atmospheric chemistry integration package and chemical reaction databas, Comput. Phys., Comm., 105, 197–215, 1997.

Chatfield, R. B., Guan, H., Thompson, A. M., and Witte, J. C.: Convective lofting links Indian Ocean air pollution to paradoxical South Atlantic ozone maxima, Geophys. Res. Lett., 31, L06103, doi:doi:10.1029/2003GL018866, 2004.

Christian, H. J., Blakeslee, R. J., Boccippio, D. J., et al.: Global frequency and distribution of lightning as observed from space by the optical transient detector, J. Geophys. Res., 108, 4005, doi:10.1029/2002JD002347, 2003.

Clerbaux, C., George, M., Turquety, S., Walker, K. A., Barret, B., Bernath, P., Boone, C., Borsdorff, T., Cammas, J. P., Catoire, V., Coffey, M., Coheur, P.-F., Deeter, M., De Mazière, M., Drummond, J., Duchatelet, P., Dupuy, E., de Zafra, R., Eddounia, F., Edwards, D. P., Emmons, L., Funke, B., Gille, J., Griffith, D. W. T., Hannigan, J., Hase, F., Höpfner, M., Jones, N., Kagawa, A., Kasai, Y., Kramer, I., Le Flochmoën, E., Livesey, N. J., López-Puertas, M., Luo, M., Mahieu, E., Murtagh, D., Nédélec, P., Pazmino, A., Pumphrey, H., Ricaud, P., Rinsland, C. P., Robert, C., Schneider, M., Senten, C., Stiller, G., Strandberg, A., Strong, K., Sussmann, R., Thouret, V., Urban, J., and Wiacek, A.: CO measurements from the ACE-FTS satellite instrument: data analysis and validation using ground-based, airborne and spaceborne observations, Atmos. Chem. Phys., 8, 2569–2594, doi:10.5194/acp-8-2569-2008, 2008.

DeCaria, A. J., Pickering, K. E., Stenchikov, G. L., and Ott, L. E.: Lightning-generated NO_x and its impact on tropospheric ozone production: a 3-D modeling study of a STERAO – a thunderstorm, J. Geophys. Res., 110, D14303, doi:10.1029/2004/JD005556, 2005.

Dentener, F., van Weele, M., Krol, M., Houweling, S., and van Velthoven, P.: Trends and inter-annual variability of methane emissions derived from 1979–1993 global CTM simulations, Atmos. Chem. Phys., 3, 73–88, doi:10.5194/acp-3-73-2003, 2003.

Dentener, F., Stevenson, D., Cofala, J., Mechler, R., Amann, M., Bergamaschi, P., Raes, F., and Derwent, R.: The impact of air pollutant and methane emission controls on tropospheric ozone and radiative forcing: CTM calculations for the period 1990–2030, Atmos. Chem. Phys., 5, 1731–1755, doi:10.5194/acp-5-1731-2005, 2005.

Doherty, R. M., Stevenson, D. S., Collins, W. J., and Sanderson, M. G.: Influence of convective transport on tropospheric ozone and its precursors in a chemistry-climate model, Atmos. Chem. Phys., 5, 3205–3218, doi:10.5194/acp-5-3205-2005, 2005.

Emanuel, K. A.: A scheme for representing cumulus convection in large-scale models, J. Atmos. Sci., 48, 2313–2335, 1991.

Emanuel, K. A.: A cumulus representation based on the episodic mixing model: the importance of mixing and microphysics in predicting humidity, AMS Meteorol. Monogr., 24(46), 185–192, 1993.

Folkins, I., Bernath, P., Boone, C., Donner, L. J., Eldering, A., Lesins, G., Martin, R. V., Sinnhuber, B.-M., and Walker, K.: Testing convective parameterizations with tropical measurements of HNO_3, CO, H_2O, and O_3: implications for the water vapor budget, J. Geophys. Res., 111, D23304, doi:10.1029/2006JD007325, 2006.

Fu, Q.: An accurate parameterization of the solar radiative properties of cirrus clouds for climate models, J. Climate, 9, 2058–2082, 1996.

Giannakopoulos, C., Chipperfield, T. P., Law, K. S., et al.: Validation and intercomparison of wet and dry deposition schemes using Pb-210 in a global three-dimensional off-line chemical transport model, J. Geophys. Res., 104, 23761–23784, 1999.

Hastenrath, S.: Climate Dynamics of the Tropics, Kluwer Academic Publishers, Dordrecht, The Netherlands, 190–200, 1991.

Hauglustaine, D. A., Hourdin, F., Jourdain, L., et al.: Interactive chemistry in the Laboratoire de Meteorologie Dynamique general circulation model: description and background tropospheric chemistry evaluation, J. Geophys. Res., 109, D04314, doi:10.1029/2003JD003957, 2004.

Heymsfield, A. J. and McFarquhar, G. M.: High albedos of cirrus in the tropical pacific warm pool: microphysical interpretations from CEPEX and from Kwajalein, Marshall Islands, J. Atmos. Sci., 53, 2424–2451, 1996.

Hourdin, F. and Armengaud, A.: The use of finite-volume methods for atmospheric advection of trace species. Part I: Test of various formulations in a general circulation model, Mon. Weather Rev., 127, 822–837, 1999.

Hourdin, F., Musat, I., Bony, S., et al.: The LMDZ4 general circulation model: climate performance and sensitivity to parametrized physics with emphasis on tropical convection, Clim. Dynam., 27, 787–813, 2006.

Huntrieser, H., Schlager, H., Feigl, C., and Höller, H.: Transport and production of NO_x in electrified thunderstorms: survey of previous studies and new observations at mid-latitudes, J. Geophys. Res., 28247–28264, 1998.

Janicot, S., Thorncroft, C. D., Ali, A., Asencio, N., Berry, G., Bock, O., Bourles, B., Caniaux, G., Chauvin, F., Deme, A., Kergoat, L., Lafore, J.-P., Lavaysse, C., Lebel, T., Marticorena, B., Mounier, F., Nedelec, P., Redelsperger, J.-L., Ravegnani, F., Reeves, C. E., Roca, R., de Rosnay, P., Schlager, H., Sultan, B., Tomasini, M., Ulanovsky, A., and ACMAD forecasters team: Large-scale overview of the summer monsoon over West Africa during the AMMA field experiment in 2006, Ann. Geophys., 26, 2569–2595, 2008, http://www.ann-geophys.net/26/2569/2008/.

Jenkins, G. S. and Ryu, J.-H.: Space-borne observations link the tropical atlantic ozone maximum and paradox to lightning, Atmos. Chem. Phys., 4, 361–375, doi:10.5194/acp-4-361-2004, 2004.

Josse, B., Simon, P., and Peuch, V.-H.: Radon global simulations with the multiscale chemistry transport model MOCAGE, Tellus B, 56, 339–356, 2004.

Jourdain, L. and Hauglustaine, D. A.: The global distribution of lightning NO_x simulated on-line in a general circulation model, Phys. Chem. Earth, 26, 585–591, 2001

Labrador, L. J., von Kuhlmann, R., and Lawrence, M. G.: The effects of lightning-produced NO_x and its vertical distribution on atmospheric chemistry: sensitivity simulations with MATCH-MPIC, Atmos. Chem. Phys., 5, 1815–1834, doi:10.5194/acp-5-1815-2005, 2005.

Law, K. S., Plantevin, P., Shallcross, D., Rogers, H., Pyle, J., Grouhel, C., Thouret, V., and Marenco, A.: Evaluation of modeled O_3 using Measurement of Ozone by Airbus In-Service Aircraft (MOZAIC) data, J. Geophys. Res., 103, 25721–25737, 1998.

Law, K. S., Fierli, F., Cairo, F., Schlager, H., Borrmann, S., Streibel, M., Real, E., Kunkel, D., Schiller, C., Ravegnani, F., Ulanovsky, A., d'Amato, F., Viciani, S., and Volk, C. M.: Air mass origins influencing TTL chemical composition over West Africa during 2006 summer monsoon, Atmos. Chem. Phys. Discuss., 10, 15485–15536, doi:10.5194/acpd-10-15485-2010, 2010.

Lawrence, M. G., von Kuhlmann, R., Salzmann, M., and Rasch, P. J.: The balance of effects of deep convective mixing on tropospheric ozone, Geophys. Res. Lett., 30, 1940, doi:10.1029/2003GL017644, 2003.

Lawrence, M. G. and Salzmann, M.: On interpreting studies of tracer transport by deep cumulus convection and its effects on atmospheric chemistry, Atmos. Chem. Phys., 8, 6037–6050, doi:10.5194/acp-8-6037-2008, 2008.

Lebel, T., Parker, D. J., Flamant, C., Bourles, B., Marticorena, B., Mougin, E., Peugeot, C., Diedhiou, A., Haywood J. M., Ngamini J. B., et al.: The AMMA field campaigns: multiscale and multidisciplinary observations in the West African region, Q. J. Roy. Meteor. Soc., 136, 8–33, 2010.

Lefevre, F., Brasseur, G. P., Folkins, I., Smith, A. K., and Simon, P.: Chemistry of the 1991/1992 stratospheric winter: threedimensional model simulations, J. Geophys. Res., 99, 8183–8195, 1994.

Liousse, C., Guillaume, B., Grégoire, J. M., Mallet, M., Galy, C., Pont, V., Akpo, A., Bedou, M., Castéra, P., Dungall, L., Gardrat, E., Granier, C., Konaré, A., Malavelle, F., Mariscal, A., Mieville, A., Rosset, R., Serça, D., Solmon, F., Tummon, F., Assamoi, E., Yoboué, V., and Van Velthoven, P.: Western african aerosols modelling with updated biomass burning emission inventories in the frame of the AMMA-IDAF program, Atmos. Chem. Phys. Discuss., 10, 7347–7382, doi:10.5194/acpd-10-7347-2010, 2010.

Livesey, N. J., Filipiak, M. J., Froidevaux, L., et al.: Validation of aura microwave limb sounder O_3 and CO observations in the upper troposphere and lower stratosphere, J. Geophys. Res., 113, D15S02, doi:10.1029/2007JD008805, 2008.

Louis, J.-F.: A parametric model of vertical eddy-fluxes in the atmosphere, Bound-Lay. Meteorol., 17, 187–202, 1979.

Mari, C., Jacob, D. J., and Bechtold, P.: Transport and scavenging of soluble gases in a deep convective cloud, J. Geophys. Res., 105, 22255–22267, 2000.

Mari, C. and Prospero, J.: African Monsoon Multidisciplinary Analysis-Atmospheric Chemistry (AMMA-AC): a new IGAC task; IGACtivities Newsletter, 31, 2–13, 2005.

Mari, C., Chaboureau, J. P., Pinty, J. P., Duron, J., Mascart, P., Cammas, J. P., Gheusi, F., Fehr, T., Schlager, H., Roiger, A., Lichtenstein, M., and Stock, P.: Regional lightning NO_x sources during the TROCCINOX experiment, Atmos. Chem. Phys., 6, 5559–5572, doi:10.5194/acp-6-5559-2006, 2006.

Mari, C. H., Cailley, G., Corre, L., Saunois, M., Attié, J. L., Thouret, V., and Stohl, A.: Tracing biomass burning plumes from the Southern Hemisphere during the AMMA 2006 wet season experiment, Atmos. Chem. Phys., 8, 3951–3961, doi:10.5194/acp-8-3951-2008, 2008.

Martin, R. V., Jacob, D. J., Logan, J. A., et al.: Interpretation of TOMS observations of tropical tropospheric ozone with a global model and in situ observations, J. Geophys. Res., 107, 4351, doi:10.1029/2001JD001480, 2002.

Marufu, L., Dentener, F., Lelieveld, J., Andreae, M. O., and Helas, G.: Photochemistry of the African troposphere: Influence of biomass-burning emissions, J. Geophys. Res., 105, 14513–14530, 2000.

Meijer, E. W., van Velthoven, P. F. J., Brunner, D. W., et al.: Improvement and evaluation of the parameterisation of nitrogen oxide production by lightning, Phys. Chem. Earth, 26, 577–583, 2001.

Michalon, N., Nassif, A., Saouri, T., et al.: Contribution to the climatological study of lightning, Geophys. Res. Lett., 26, 3097–3100, 1999

Nedelec, P., Cammas, J.-P., Thouret, V., Athier, G., Cousin, J.-M., Legrand, C., Abonnel, C., Lecoeur, F., Cayez, G., and Marizy, C.: An improved infrared carbon monoxide analyser for routine measurements aboard commercial Airbus aircraft: technical validation and first scientific results of the MOZAIC III programme, Atmos. Chem. Phys., 3, 1551–1564, doi:10.5194/acp-3-1551-2003, 2003.

Ordóñez, C., Elguindi, N., Stein, O., Huijnen, V., Flemming, J., Inness, A., Flentje, H., Katragkou, E., Moinat, P., Peuch, V.-H., Segers, A., Thouret, V., Athier, G., van Weele, M., Zerefos, C. S., Cammas, J.-P., and Schultz, M. G.: Global model simulations of air pollution during the 2003 European heat wave, Atmos. Chem. Phys., 10, 789–815, doi:10.5194/acp-10-789-2010, 2010.

Pickering, K. E., Wang, Y., Tao, W. K., Price, C., and Muller, J. F.: Vertical distributions of lightning NO_x for use in regional and

global chemical transport models, J. Geophys. Res., 103, 31203–31216, doi:10.1029/98JD02651, 1998.

Pradier, S., Attie, J.-L., Chong, M., et al.: Evaluation of 2001 springtime CO transport over West Africa using MOPITT CO measurements assimilated in a global chemistry transport model, Tellus B, 58, 163–176, 2006.

Prather, M. J.: Numerical advection by conservation of 2nd order moments, J. Geophys. Res., 91, 6671–6681, 1986.

Price, C. and Rind, D.: A simple lightning parametrization for calculating global lightning distributions, J. Geophys. Res., 97, 9919–9933, 1992.

Price, C. and Rind, D.: What determines the cloud-to-ground lightning fraction in thunderstorms, Geophys. Res. Lett., 20, 463–466, 1993.

Price, C., Penner, J., and Prather, M.: NO_X from lightning. 1. Global distribution based on lightning physics, J. Geophys. Res., 102, 5929–5941, 1997.

Pumphrey, H. C., Filipiak, M. J., Livesey, N. J., et al.: Validation of middle-atmosphere carbon monoxide retrievals from MLS on Aura, J. Geophys. Res., 112, D24S38, doi:10.1029/2007JD008723,2007.

Rasch, P. J., Feichter, J., and Law, K.: A comparison of scavenging and deposition processes in global models: results from the WCRP Cambridge Workshop of 1995, Tellus B, 52, 1025–1056, 2000.

Real, E., Orlandi, E., Law, K. S., Fierli, F., Josset, D., Cairo, F., Schlager, H., Borrmann, S., Kunkel, D., Volk, C. M., McQuaid, J. B., Stewart, D. J., Lee, J., Lewis, A. C., Hopkins, J. R., Ravegnani, F., Ulanovski, A., and Liousse, C.: Cross-hemispheric transport of central African biomass burning pollutants: implications for downwind ozone production, Atmos. Chem. Phys., 10, 3027–3046, doi:10.5194/acp-10-3027-2010, 2010.

Redelsperger, J. L., Thorncroft, C. D., Diedhiou, A., et al.: African monsoon multidisciplinary analysis – an international research project and field campaign, B. Am. Soc., 87, 1739–1746, 2006.

Reeves, C. E., Formenti, P., Afif, C., Ancellet, G., Attie, J.-L., Bechara, J., Borbon, A., Cairo, F., Coe, H., Crumeyrolle, S., Fierli, F., Flamant, C., Gomes, L., Hamburger, T., Lambert, C., Law, K. S., Mari, C., Matsuki, A., Methven, J., Mills, G. P., Minikin, A., Murphy, J. G., Nielsen, J. K., Oram, D. E., Parker, D. J., Richter, A., Schlager, H., Schwarzenboeck, A., and Thouret, V.: Chemical and aerosol characterisation of the troposphere over West Africa during the monsoon period as part of AMMA, Atmos. Chem. Phys. Discuss., 10, 7115–7183, doi:10.5194/acpd-10-7115-2010, 2010.

Ridley, B. A., Pickering, K. E., and Dye, J. E.: Comments on the parameterization of lightning-produced NO in global chemistry-transport models, Atmos. Environ., 39, 6184–6187, 2005

Rossow, W. B., Walker, A. W., Beuschel, D. E., and Roiter, M. D.: International Satellite Cloud Climatology Project (ISCCP) Documentation of New Cloud Datasets. WMO/TD-No. 737, World Meteorological Organization, 115 pp., 1996.

Sander, S. P., Friedl, R. R., Ravishankara, A. R., et al.: Chemical Kinetics and Photochemical Data for Use in Atmospheric studies, Evaluation No. 15, JPL Publication 06–2, 2006.

Saunois, M., Mari, C., Thouret, V., et al.: An idealized two-dimensional approach to study the impact of the West African monsoon on the meridional gradient of tropospheric ozone, J. Geophys. Res., 113, D07306, doi:10.1029/2007JD008707, 2008.

Saunois, M., Reeves, C. E., Mari, C. H., Murphy, J. G., Stewart, D. J., Mills, G. P., Oram, D. E., and Purvis, R. M.: Factors controlling the distribution of ozone in the West African lower troposphere during the AMMA (African Monsoon Multidisciplinary Analysis) wet season campaign, Atmos. Chem. Phys., 9, 6135–6155, doi:10.5194/acp-9-6135-2009, 2009.

Sauvage, B., Thouret, V., Cammas, J.-P., Gheusi, F., Athier, G., and Nédélec, P.: Tropospheric ozone over Equatorial Africa: regional aspects from the MOZAIC data, Atmos. Chem. Phys., 5, 311–335, doi:10.5194/acp-5-311-2005, 2005.

Sauvage, B., Thouret, V., Cammas, J.-P., Brioude, J., Nedelec, P., and Mari, C.: Meridional ozone gradients in the African upper troposphere, Geophys. Res. Lett., 34, L03817, doi:10.1029/2006GL028542, 2007a.

Sauvage, B., Gheusi, F., Thouret, V., Cammas, J.-P., Duron, J., Escobar, J., Mari, C., Mascart, P., and Pont, V.: Medium-range mid-tropospheric transport of ozone and precursors over Africa: two numerical case studies in dry and wet seasons, Atmos. Chem. Phys., 7, 5357–5370, doi:10.5194/acp-7-5357-2007, 2007b.

Sauvage, B., Martin, R. V., van Donkelaar, A., and Ziemke, J. R.: Quantification of the factors controlling tropical tropospheric ozone and the South Atlantic maximum, J. Geophys. Res., 112, D11309, doi:10.1029/2006JD008008, 2007c.

Schlager, H., Konopka, P., Schulte, P., Schumann, U., Ziereis, H., Arnold, F., Klemm, M., Hagen, D., Whitefield, P., and Ovarlez, J.: In situ observations of air traffic emission signatures in the North Atlantic flight corridor, J. Geophys. Res., 102, 10739–10750, 1997.

Schumann, U. and Huntrieser, H.: The global lightning-induced nitrogen oxides source, Atmos. Chem. Phys., 7, 3823–3907, doi:10.5194/acp-7-3823-2007, 2007.

Shindell, D. T., Faluvegi, G., Stevenson, D. S., et al.: Multimodel simulations of carbon monoxide: comparison with observations and projected near-future changes, J. Geophys. Res., 111, D19306, doi:10.1029/2006JD007100, 2006.

Stevenson, D. S., Dentener, F. J., Schultz, M. G., et al.: Multimodel ensemble simulations of present-day and near-future tropospheric ozone, J. Geophys. Res., 111, D08301, doi:10.1029/2005JD006338, 2006.

Stockwell, W. R., Kirchner, F., Khun, M., and Seefeld, S.: A new mechanism for regional atmospheric chemistry modelling, J. Geophys. Res., 102, 25847–25879, 1997.

Stockwell, D. Z., Giannakopoulos, C., Plantevin, P. H., et al.: Modelling NO_X from lightning and its impact on global chemical fields, Atmos. Environ., 33, 4477–4493, 1999.

Teyssédre, H., Michou, M., Clark, H. L., Josse, B., Karcher, F., Olivié, D., Peuch, V.-H., Saint-Martin, D., Cariolle, D., Attié, J.-L., Nédélec, P., Ricaud, P., Thouret, V., van der A, R. J., Volz-Thomas, A., and Chéroux, F.: A new tropospheric and stratospheric Chemistry and Transport Model MOCAGE-Climat for multi-year studies: evaluation of the present-day climatology and sensitivity to surface processes, Atmos. Chem. Phys., 7, 5815–5860, doi:10.5194/acp-7-5815-2007, 2007.

Thery, C., Laroche, P., and Blanchet, P.: Lightning activity during EULINOX and estimations of NO_X production by flashes, EULINOX – The European Lightning Nitrogen Oxides Experiment, No. 2000–28, DLR Forschungsbericht, DLR, Köln, 129–145, 2000.

Thompson, A., Doddridge, B., Witte, J., Hudson, R., Luke, W.,

Johnson, J., Johnson, B., Oltmans, S., and Weller, R.: A tropical atlantic paradox: shipboard and satellite views of a tropospheric ozone maximum and wave-one in January–February 1999, Geophys. Res. Lett., 27, 3317–3320, 2000.

Thouret, V., Marenco, A., Logan, J. A., Nedelec, P., and Grouhel, C.: Comparisons of ozone measurements from the MOZAIC airborne program and the ozone sounding network at eight locations, J. Geophys. Res., 103(D19), 25695–25720, 1998.

Tiedtke, M.: A comprehensive mass flux scheme for cumulus parameterization in large-scale models, Mon. Weather. Rev., 117, 1779–1800, 1989.

Tost, H., Jöckel, P., and Lelieveld, J.: Lightning and convection parameterisations – uncertainties in global modelling, Atmos. Chem. Phys., 7, 4553–4568, doi:10.5194/acp-7-4553-2007, 2007.

Tost, H., Lawrence, M. G., Brühl, C., Jöckel, P., The GABRIEL Team, and The SCOUT-O3-DARWIN/ACTIVE Team: Uncertainties in atmospheric chemistry modelling due to convection parameterisations and subsequent scavenging, Atmos. Chem. Phys., 10, 1931–1951, doi:10.5194/acp-10-1931-2010, 2010.

van der Werf, G. R., Randerson, J. T., Giglio, L., Collatz, G. J., Kasibhatla, P. S., and Arellano Jr., A. F.: Interannual variability in global biomass burning emissions from 1997 to 2004, Atmos. Chem. Phys., 6, 3423–3441, doi:10.5194/acp-6-3423-2006, 2006.

Van Leer, B., Towards the ultimate conservative difference scheme. Part IV: A new approach to numerical convection, J. Comput. Phys., 23, 276–299, 1977.

Wang, K. Y., Pyle, J. A., Sanderson, M. G., et al.: Implementation of a convective atmospheric boundary layer scheme in a tropospheric chemistry transport model, J. Geophys. Res., 104, 23729–23745, 1999.

Williams, J. E., Scheele, M. P., van Velthoven, P. F. J., Cammas, J.-P., Thouret, V., Galy-Lacaux, C., and Volz-Thomas, A.: The influence of biogenic emissions from Africa on tropical tropospheric ozone during 2006: a global modeling study, Atmos. Chem. Phys., 9, 5729–5749, doi:10.5194/acp-9-5729-2009, 2009a.

Williams, J. E., Bouarar, I., Josse, B., et al.: Global Chemistry simulations in the AMMA-Model Intercomparison project, B. Am. Meteorol. Soc., 91, 611–624, 2009b.

Williams, J. E., Scheele, M. P., van Velthoven, P. F. J., Thouret, V., Saunois, M., Reeves, C. E., and Cammas, J.-P.: The influence of biomass burning on tropospheric composition over the tropical Atlantic Ocean and Equatorial Africa during the West African monsoon in 2006, Atmos. Chem. Phys. Discuss., 10, 7507–7552, doi:10.5194/acpd-10-7507-2010, 2010.

Waters, J. W., et al.: The Earth Observing System Microwave Limb Sounder (EOS MLS) on the Aura satellite, IEEE T. Geosci. Remote, 44, 1075–1092, 2006.

Yang, X., Cox, R. A., Warwick, N. J., Pyle, J. A., Carver, G. D., O'Connor, F. M., and Savage, N. H.: Tropospheric bromine chemistry and its impacts on ozone: a model study, J. Geophys. Res., 110, D23311, doi:10.1029/2005JD006244, 2005.

Yarwood, G., Rao, S., Yocke, M., and Whitten, G. Z.: Updates to the Carbon Bond Mechanism: CB05, Yocke and company, Final Report, RT-04–00675, available online at: http://www.camx.com/publ/, 2005.